Understanding Extreme Precipitation Behaviour in British Columbia's Lower Mainland Using Historical and Proxy Records

by

Christina Spry

B.Sc. (Earth Sciences), St. Francis Xavier University, 2008

Research Project Submitted in Partial Fulfillment of the
Requirements for the Degree of
Master of Resource Management

in the
School of Resource and Environmental Management
Faculty of Environment

SIMON FRASER UNIVERSITY

Fall 2013

Approval

Name: **Christina Spry**

Degree: **Master of Resource Management**

Report No.: **527**

Title: ***Understanding extreme precipitation behaviour in British Columbia's Lower Mainland using historical and proxy records***

Examining Committee: **Chair:** Thomas Rodengen
PhD Candidate

Karen Kohfeld
Senior Supervisor
Associate Professor

Ken Lertzman
Supervisor
Professor

Diana Allen
Supervisor
Department of Earth Sciences

Date Defended/Approved: September 4, 2013

Partial Copyright Licence

Abstract

In British Columbia, Pineapple Express storms can lead to flooding, slope failures and negative impacts to water quality. Mitigating the impacts of extreme weather events in a changing climate requires an understanding of how local climate responds to regional-to-global climate forcing patterns. In this study, I use historical and proxy data to identify the distinguishing characteristics of Pineapple Express storms and to develop a tree ring oxygen isotope record (1960-1995) of local climate conditions in the Lower Mainland of British Columbia. I found that high magnitude Pineapple Express storms have significantly higher precipitation and streamflow than other storms types, which result in relatively high contributions of Pineapple Express storms to the annual water budget. As well, Pineapple Express precipitation is characterized by an enriched $\delta^{18}O$ isotopic signature when compared to precipitation originating from the North Pacific Ocean. However, differences in source water do not appear to be driving the variability in tree ring $\delta^{18}O$ ratios. Instead, tree ring isotopic values exhibit a regional climate pattern that is strongly driven by latitudinal temperature gradients and the Rayleigh distillation effect. Therefore, future warmer conditions may decrease the temperature gradient between the equator and the poles, which can be recorded in the tree ring isotope record. The results also suggest that warmer temperatures due to climate change could result in more active Pineapple Express storm seasons, with multiple PE storms happening over a short period of time. Concurrent storms significantly increase the risk to society because the resulting antecedent saturated soil conditions can trigger precipitation-induced natural hazards.

Keywords: extreme weather; stable isotopes; Pineapple Express; British Columbia; climate change; tree rings

To my parents, Jon and Laura,

for their unconditional love and support.

I couldn't have done this without you.

Acknowledgements

First, I would like to thank the members of my dedicated supervisory committee, Karen Kohfeld, Ken Lertzman, and Diana Allen for their continuous support and guidance. I respect and admire all of you greatly, so it was a pleasure to work with you closely and get to know you on a personal level. Thanks to David Dunkley and Metro Vancouver for the valuable input and allowing me access to the beautiful Capilano Watershed in North Vancouver. I would also like to acknowledge Henri Grissino-Mayer and Zheng-hua Li for their professional advice and mentoring. Numerous others contributed to this project by providing their data and sharing their expertise, so thanks to Michael Dettinger, Roderick Bale, Trevor Porter, Dinka Besic and Andy Cooper, and to my friends in the COPE lab, especially Celeste Barlow, Liz Sutton, and Joseph Bailey.

This project was supported by a Simon Fraser University Community Trust Endowment Fund grant to Diana Allen, Ken Lertzman and Karen Kohfeld, as well as Karen Kohfeld's NSERC Canada Research Chair program and NSERC Discovery Grant.

Table of Contents

List of Tables

List of Figures

List of Acronyms

$\delta^{18}O$	^{18}O: ^{16}O isotopic ratio measure
AO	Arctic Oscillation
AR	Atmospheric River
BC	British Columbia
CA	California
CRCM	Canadian Regional Climate Model
CSO	Combined Sewer Overflow
CWH	Coastal Western Hemlock Biogeoclimatic Zone
DF	Douglas-fir
ENSO	El Niño Southern Oscillation
EW	Earlywood
FVFP	Fraser Valley Fire Period
GNIP	Global Network for Isotopes in Precipitation
IPCC	Intergovernmental Panel on Climate Change
K	Hydraulic conductivity
LW	Latewood
MJO	Madden Julian Oscillation
NCEP	National Centers for Environmental Prediction
PNA	Pacific/North American teleconnection
NPGO	North Pacific Gyre Oscillation
NWT	Northwest Territories
p	Atmospheric pressure
P	Precipitation
PDO	Pacific Decadal Oscillation
PE	Pineapple Express
Q	Infiltration rate
SSO	Sanitary Sewer Overflow
SST	Sea Surface Temperature
T	Temperature
u	Wind speed
US	United States
V-SMOW	Vienna Standard Mean Ocean Water
WA	Washington

Chapter 1.

General Introduction

Global ocean-atmosphere conditions are expected to change as the climate system responds to rapid inputs of carbon dioxide into the atmosphere (Intergovernmental Panel on Climate Change (IPCC), 2013). Changes in precipitation and temperature regimes due to climate change are creating a “new normal”, one which could place unexpected strain on our existing societal structures. For example, increases in the frequency and magnitude of extreme weather events put additional pressure on aging wastewater infrastructure which could overflow and contaminate local waterways. In British Columbia, some of the most severe storm impacts result from Pineapple Express storms, a rare but powerful subtropical storm system that often causes widespread precipitation and flooding (Dettinger, 2004). The storms are distinguishable based on their atmospheric river configuration; however, their low frequency of occurrence has made it difficult to study their long-term patterns and impacts. The original objective of my research was to fill this void by developing a chronology of Pineapple Express storms events for Vancouver, British Columbia (BC), which could then be compared to meteorological, natural hazard and public health records.

Based on new Pineapple Express and stable isotope dendrochronology research (Miller et al., 2006; Dettinger, 2004; Berkelhammer and Stott, 2008), a work plan was devised to develop a tree ring oxygen isotope record for Vancouver, BC and use it a proxy for past occurrences of Pineapple Express (PE) storms. Miller et al. (2006) demonstrated that $\delta^{18}O$ values from the α-cellulose in the tree rings of Georgian longleaf pine provide accurate records of historical tropical cyclone activity along the Atlantic seaboard. My goal was to apply similar methods to studying PE storms on the West Coast. Oxygen isotope measurements made on precipitation samples that I collected during storm events suggested Vancouver PE storms are substantially enriched in $\delta^{18}O$

compared with storms originating in the North Pacific. The first objective of this research was to test whether the oxygen isotope content of Douglas-fir tree rings would similarly record the source water changes reflected in these storms. Dettinger (2004) developed a chronology of PE events (1948-1999) using historical water vapour transport rates, which could be cross-referenced with tree ring data from Vancouver. My initial comparisons between the $\delta^{18}O$ of storms precipitation from PE and North Pacific storms revealed a substantial difference in the isotopic source waters of these storms. This difference led to the first testable hypothesis that changes in the $\delta^{18}O$ of Douglas-fir tree rings could be attributed to interannual changes in the frequency and magnitude of PE storms.

My further investigations into this question revealed several important points. First, while PE storms are noted in newscasts and in public discourse, no diagnostic criteria has been established for understanding the nature, frequency, and impact of these storms in the Lower Mainland of BC. Second, using the one record of PE storm activity available for the Lower Mainland (Dettinger, 2004), correlations between the Douglas-fir $\delta^{18}O$ and PE storm activity between 1960-1995 suggested that the tree ring $\delta^{18}O$ record was driven more strongly by regional climatic conditions rather than individual PE storms. The results suggested that further research was required to decipher which key parameters might influence tree ring $\delta^{18}O$ variability in Vancouver. It was at this point that I chose to move forward with two separate papers: the first on characteristics of Pineapple Express storms and the second one investigating the drivers of tree ring stable isotope variability.

In Chapter 2, I use meteorological, streamflow and isotope data to identify the distinguishing characteristics of PE storms making landfall in coastal BC. PE storms are subtropical winter storms that often lead to precipitation-induced natural hazards (Dettinger, 2004), yet they have not been well studied in the Lower Mainland. Their subtropical moisture source differentiates them from other types of winter storms that originate in the North Pacific Ocean (Berkelhammer and Stott, 2008), and my research aims to quantify and compare those differences. The spatial variability in the isotopic composition of global precipitation is largely temperature dependent, and warm air masses tend to hold moisture that is isotopically heavier than air masses in cooler regions (Dansgaard, 1964; Rozanski et al., 1992). Therefore, oxygen isotopes can be a

very useful tool for identifying, tracking and analyzing the characteristics of individual storm patterns, and for informing climate change research. Climate change is expected to increase the frequency and magnitude of extreme weather events (Yin, 2005; Jakob and Lambert, 2009), however it is not likely that storm patterns from distinct geographic regions will evolve at the same rate or by the same magnitude. I use meteorological and hydrometric station data to explore trends in the frequency and magnitude of past PE events from 1948-2007 and identify specific examples of impacts to local water resources.

In Chapter 3, I present annual and seasonal (i.e., earlywood, latewood) Douglas-fir $\delta^{18}O$ records for Vancouver, BC (1960-1995) and identify potential drivers of isotopic variability within those records. The relative abundance of $\delta^{18}O$ in tree rings is influenced by a variety of factors, including temperature, precipitation, moisture source, storm trajectory, soil conditions, tree physiology, and more (Dansgaard, 1964; Gat, 1996; Lee and Fung, 2008), so identifying key variables is often challenging. Using meteorological station data and climate indices, I investigate the relationships between the measured tree ring isotope values and temperature, precipitation, and oscillatory climate behaviour in the Pacific Northwest. In addition, I compare the annual $\delta^{18}O$ tree ring record to other records from across the west coast of North America, from California (Bale et al., 2010) up to the Northwest Territories (Porter et al., 2009). Geographic comparisons help to place the BC record in context, and help to establish whether or not the isotopic ratios reflect large-scale regional climate patterns. The California and Northwest Territories records are substantially longer than the BC record, so identifying any significant relationships between geographic regions can help leverage our results and extrapolate the BC record further back in time.

Both chapters explore new ways of understanding the regional climate of British Columbia using historical and proxy data, and build upon a solid foundation of new advancements in paleoclimate research. The overarching theme is that making informed decisions about the future requires a sound understanding of the past. Quantifying the extent of ongoing and future changes in extreme precipitation requires detailed records of historical conditions. For example, using these records to distinguish between cyclical behaviour and unprecedented trends helps to resolve the underlying causes in extreme events. The more information we know about historical conditions, the more we can

resolve about the causes and impacts. In this study, the tree ring δ18O record from coastal BC was not a good proxy for the occurrence of Pineapple Express storms in the region. However, the record did provide insight into historical regional climate conditions. As well, I have identified the value in establishing an ongoing chronology of new Pineapple Express storms that can track storm characteristics, inform emergency management policy and mitigate physical, societal and economic impacts. Oxygen isotope composition of storm precipitation can be used to identify storm types, establish a chronology of events, and compare the results to other data sets and the occurrence of particular societal impacts. This research project is relevant to resource managers because it sits at the nexus of science and policy, and demonstrates how scientific research can be used to understand where and how to invest our limited resources and mitigate the most severe impacts of extreme weather events in BC.

1.1. References

Bale, R. J. , I. Robertson, S. W. Leavitt, N. J. Loader, T. P. Harlan, M. Gagen, G. H. F. Young, A. Z. Csank, C. A. Froyd and D. McCarroll. 2010. Temporal stability in bristlecone pine tree-ring stable oxygen isotope chronologies over the last two centuries. *The Holocene* 20: 3-6.

Berkelhammer, M. B. and L. D. Stott. 2008. Recent and dramatic changes in Pacific storm trajectories recorded in $\delta^{18}O$ from Bristlecone Pine tree ring cellulose. *Geochemistry, Geophysics, Geosystems* 9:Q04008.

Dansgaard, W. 1964. Isotopes in precipitation. *Tellus* 16:4.

Dettinger, M. 2004. *Fifty-two years of "Pineapple-Express" storms across the west coast of North America.* California: United States Geological Survey, Scripps Institutions of Oceanography for the California Energy Commission, PIER Energy-Related Environmental Research, CEC-500-2005-004.

Gat, J. 1996. Oxygen and hydrogen isotopes in the hydrologic cycle. *Annual Review Earth Planetary Sciences* 24: 225–62.

IPCC. 2013. Summary for Policy Makers. In *Climate Change 2013: The Physical Science Basis.* Contribution of Working Group I to the Fifth Assessment Report of the Intergovernmental Panel on Climate Change, ed. T. F. Stocker, D. Qin, G. K. Plattner, M. Tignor, S. K. Allen, J. Boschung, A. Nauels, Y. Xia, V. Bex, and P. M. Midgley. Cambridge University Press, Cambridge, United Kingdom and New York, NY, USA.

Jakob, M. and S. Lambert. 2009. Climate change effects on landslides along the southwest coast of British Columbia. *Geomorphology* 107(3-4): 275-284.

Lee, J. E. and I. Fung. 2008. "Amount effect" of water isotopes and quantitative analysis of post-condensation processes. *Hydrological Processes* 22:1-8.

McCarroll, D. and N. J. Loader. 2004. Stable isotopes in tree rings. *Quaternary Science Review* 23:771-801.

Miller, D. L., C. I. Mora, H. D. Grissino-Mayer, C. J. Mocks, M. E. Uhle and Z. Sharp. 2006. Tree-ring isotope records of tropical cyclone activity, *Proceedings of the National Academy of Science USA* 103(39): 14294-14297.

Porter, T. J., M. F. J. Pisaric, S. V. Kokelj, and T. W. D. Edwards. 2009. Climate signals in δ13C and δ18O of tree-rings from white spruce in the Mackenzie Delta region, northern Canada. *Arctic, Antarctic, and Alpine Research* 41: 497-505.

Rozanski, K., L. Araguasaraguas and R. Gonfiantini. 1992. Relationship between long-term trends of O-18 isotope composition of precipitation and climate. *Science* 258(5084): 981-985.

Yin, J. H. 2005. A consistent poleward shift of the storm tracks in simulations of 21st century climate. *Geophysical Research Letters* 32: L18701.

Chapter 2.

Characterizing Pineapple Express Storms in British Columbia's Lower Mainland Using Meteorological, Streamflow and Stable Isotope Data

2.1. Introduction

On November 5, 2006, a subtropical storm system made landfall at approximately 47.5°N along the west coast of North America (Dettinger, 2008). By the next day, ambient temperatures at the Vancouver International Airport meteorological station climbed 4°C to reach the peak daily mean temperature for the month at 13.9ºC. Weather stations across the south coast of British Columbia (BC) and Vancouver Island recorded intense rainfall events, receiving 50-300 mm of cumulative rainfall in two days (Emergency Management BC (EMBC), 2006a). Stream levels rose rapidly, and the BC Ministry of Environment's River Forecast Centre issued flood warnings for the Lower Fraser Valley, Greater Vancouver and the North Shore mountains. In the nearby Chilliwack River Valley, nearly 200 families were evacuated as the Chilliwack River stream flows peaked above 1000 m^3/s (Emergency Management BC, 2006a). Local residents also reported mud slides and numerous road closures (EMBC, 2006a; EMBC, 2006b). Effects from the storm were felt in the United States as well, resulting in new rainfall records, major flooding, debris flows, and highway damage across Washington and Oregon States. The heaviest rainfall amounts were recorded in the Cascades and Coast Mountains, which received 200-500 mm over three days (Neiman et al., 2008a). Many streams experienced maximum one day flows, within the top 1% of those observed historically for the month of November. Officials in Mount Rainier National Park declared the storm "the worst natural disaster in a century" (Parker, 2009), and the widespread flooding and debris flows associated with the storm led to about $50 million

in damages in the United States (National Oceanic and Atmospheric Association (NOAA, no date).

The powerful storm that created this widespread damage is known colloquially as a “Pineapple Express” (PE), a name that refers to the subtropical origins of the moisture source and the rapid vapour transport rate (Dettinger, 2004). PE storms occur approximately 0-4 times per winter across the entire latitudinal range of western North America, with the most common west coast crossing being 45ºN (Dettinger, 2004). They differ from other types of winter storms affecting coastal BC, most of which originate in the North Pacific Ocean and are associated with cold temperatures and intense snowfall (Berkelhammer and Stott, 2008; Figure 2.1). In contrast, PE storms tend to be associated with a low pressure cell over the Gulf of Alaska that funnels warm and wet subtropical air from around Hawaii to the west coast of North America (Mo, 2011). PE events are also associated with sharp temperature gradients (cold in the western Pacific and warm in the east; Dettinger, 2005) and have characteristic 500-hPa geopotential height anomalies (Lackmann and Gyakum, 1999). The mid-tropospheric pressure anomalies allow cold fronts to develop, which power PE storms and provide a persistent storm track to the north east (Ralph et al., 2005; Neiman et al., 2008a). Mid-latitude low pressure cyclones develop along this cold front and are the source of the subtropical water vapour that eventually reaches North America (Ralph et al., 2004). In satellite imagery (Figure 2.1a), this defining configuration of PE storms appears as a long and narrow band of moisture in the atmosphere, known as an “atmospheric river” (AR; Dettinger, 2004).

ARs off the west coast of North America can exceed 2,000 km in length, but are typically only a few hundred kilometres wide (Figure 2.1a; Ralph et al*.,* 2004; Neiman et al*.,* 2008a). Because of their unique structure, ARs account for >90% of the world’s water vapour transport towards the poles yet they cover <10% of the Earth’s circumference (Zhu and Newell, 1998). This condensed structure concentrates the water vapour in a narrow plume in the atmosphere, which is the key to their rapid moisture transport capabilities. The vapour is driven towards coastal BC by strong winds that occur about 2 km above the sea surface (Neiman et al*.,* 2008b). Observations from two atmospheric rivers (one in 1998, the other in 2005) indicate the average water vapour

transport rate was 13-26 km^3/day, 7.5-15 times greater than the average daily discharge of the Mississippi River (Ralph et al., 2005).

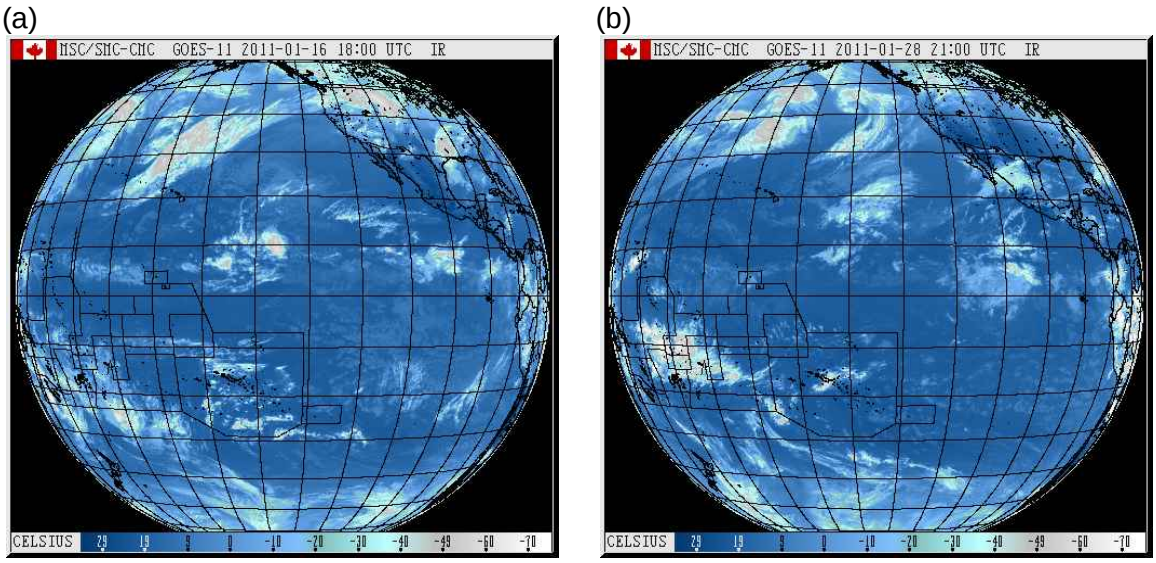

Figure 2.1. GOES-West satellite images of typical storm types affecting the western coast of North America in the winter season. (a) Classic PE storm with a subtropical moisture source and characteristic atmospheric river form (from January 16, 2011). (b) A typical winter storm from January 28, 2011, with a moisture source in the subarctic North Pacific. Images retrieved from Environment Canada's Weather Office (http://www.weatheroffice.gc.ca). The images are a copy of official work published by the Government of Canada and they have not been produced in affiliation with or with the endorsement of the Government of Canada.

PE storms are among the most dangerous and destructive weather systems to impact coastal BC. Orographic lifting associated with PE storms when they encounter the Coast Mountains can result in extreme precipitation, flooding, and rapid mass movements such as debris flows and snow avalanches (Dettinger, 2011). The warm temperatures associated with the influx of subtropical air can lead to rain-on-snow events, which amplify the potential for precipitation-induced natural hazards (Dettinger, 2004). The physical impacts of PE storms have management and policy implications that translate into real socioeconomic costs resulting from loss of life, property, infrastructure, and economic activity. PE storm flooding in northern California from December 31, 1996 to January 2, 1997 killed nine people and forced 120,000 others from their homes. Cumulative damages were assessed at almost $2 billion, resulting from flood impacts to homes, businesses, agricultural lands, bridges, roads and floodwater management

infrastructure (Junker et al., 2008; California Department of Water Resources (CDWR), 2002). Consideration of indirect costs, including a temporary disruption to the economy, catapulted the damage estimates to greater than $7 billion (CDWR, 2002). In British Columbia, PE storms can lead to issues with water quality and supply and risks to public safety from precipitation-induced natural hazards (Burrard Inlet Environmental Action Program (BIEAP), 2010; Adaptation to Climate change Team (ACT), 2011; Septer, 2007; Jakob and Weatherly, 2003).

In spite of these consequences, PE storms have not been well studied, largely because of data constraints and the lack of an established definition for what constitutes a PE storm. PE storms develop over the data-sparse Pacific Ocean, an area that relies mainly on scattered buoy data (Neiman et al., 2008a), and therefore there is often insufficient information for characterizing individual storm events. In Canada, PE storm events are not readily documented by Environment Canada's Weather Office because of a lack of specific criteria and thresholds for identification. Instead, "Pineapple Express" is used colloquially by newscasters and the public without a full understanding of PE characteristics (Parker, 2009). The lack of an established definition of a true "Pineapple Express" event hinders development of a chronology of events that would facilitate the analysis of temporal changes in PE storm frequency and magnitude. PE storms are readily recognizable as ARs from satellite imagery (e.g., Figure 2.1a); however, high resolution satellite imagery has been available only for the past few decades. The short time scales of satellite records do not provide sufficient information for analyzing PE storms in a historical context.

Dettinger (2004) made the first steps towards explicitly defining, quantifying and cataloguing historical PE storms between 1948 and 1999, using atmospheric wind and moisture pathways from the National Center for Environmental Prediction (NCEP) Reanalysis dataset. The study identified PE storms as winter storms that (a) have a direct, continuous path from the tropics at 20-25°N to 32.5-52.5°N; (b) cross the west coast of North America at 120°W; and (c) have vapour transport rates exceeding 500 kg/m/s. Using these criteria, Dettinger (2004) identified 206 PE storms between 1948 and 1999. The frequency and magnitude of storm events exhibited substantial interannual variability, although Dettinger (2004) also noted an overall increasing trend in the number of events per year (r^2= 0.18, p= 0.2).

Climate change is expected to increase the frequency and magnitude of extreme weather events (Yin, 2005; Salathé, 2006; Tebaldi et al., 2006; Salathé et al., 2008; Jakob and Lambert, 2009), which could also mean an increase in the frequency and severity of PE storms. Understanding how PE storm patterns will shift in the future is imperative if the risks to society are to be mitigated and the financial burden associated with damages minimized. However, identifying, predicting, and managing risks associated with PE storms remains a challenge for natural hazard management and public safety. The PE storm systems manifest themselves only a few times each year, with the most intense storms remaining even rarer and more unpredictable (Dettinger, 2004).

Although a single PE storm can be severe and widespread, region-specific studies of PE storms are essential, because differences in regional climate, geography, infrastructure, and policy can drastically change the degree of risk associated with extreme weather events. The majority of PE storm research to date has been conducted on storms making landfall in the United States (Burns et al., 1998; Dettinger et al., 2011; Neiman et al., 2008a), mainly due to region-specific research investments. For example, in 2006, the State of California invested $4.5 billion into flood management and state research programs, a substantial portion of which will be used to study PE storms (Dettinger, 2011). BC differs from California in terms of its overall climate, population density, building codes and standards, water supply and quality, and other factors that may influence the risk from high magnitude PE events. Therefore, while new research coming out of California is useful and informative, it does little to speak to the distinct situation in the Lower Mainland of British Columbia.

The objective of this study is to characterize PE storms affecting the Lower Mainland of BC in terms of their hydroclimatic and isotopic properties. Meteorological, streamflow and isotopic parameters can vary between storm types due to differences in moisture source, seasonality, synoptic conditions, and rain-on-snow potential. Isolating the hydroclimatic characteristics of PE storms can help resource managers better anticipate specific impacts to the Vancouver area, as well as inform the decision-making process on how to allocate limited funds to mitigate the impacts of extreme weather events and deliver the maximum benefits to society. Additionally, the isotopic signature of PE storms can be used to further refine the definition of a PE storm and be used as a

tracking tool to catalogue the arrival of different storm types in the Lower Mainland of British Columbia. This study aims to quantify these distinguishing characteristics, examine their temporal behaviour, and identify how this information can be used by resource managers to educate and guide extreme weather event hazard planning and mitigation.

2.1.1. Study Area

This study uses data from the Vancouver area (Figure 2.2; 49ºN, 123º W) as a window on the Lower Mainland of British Columbia, while also considering the broader context of PE storm occurrence in western North America. Metro Vancouver is a large urban centre that borders the Pacific Ocean, and has a population of 2.3 million people. The climate is mild and wet, with an average annual temperature of 10.1°C and mean annual precipitation of 1199 mm from 1971-2000 at the Vancouver International Airport (Environment Canada, 2012). The Coast Mountain Range surrounding the Metro Vancouver area intensifies storms through orographic enhancement (Neiman et al., 2002), creating one of the wettest climates in Canada. Nearly three quarters of the annual precipitation in the area is received over the winter season (November-March), with storm systems originating either in the North or subtropical Pacific (Berkelhammer and Stott, 2008).

Two main data collection locations were used (Figure 2.1; Table 2.2): the Vancouver International Airport and the Capilano Watershed. Together, these two sites represent the contrasting geography of the Metro Vancouver area. The Vancouver Airport is a low-lying coastal site located on the Fraser River Delta, and has a continuous and reliable meteorological record. The Capilano Watershed is a multi-use watershed located in the inland, mountainous area of North Vancouver and is the source of 33% of Metro Vancouver's drinking water supply (Metro Vancouver, 2011a). Storm precipitation samples complement the meteorological and hydrometric data, and were taken from locations in Burnaby and Vancouver (Figure 2.2; Table 2.1).

2.2. Methods

The goal of this analysis is to determine which variables distinguish PE events from other types of storms affecting the Vancouver area. The unique characteristics of PE storms were identified by examining the hydroclimatic and oxygen isotope characteristics of these storms, using meteorological station variables of temperature (T), precipitation (P), wind speed (u) and atmospheric pressure (p), streamflow data, and oxygen isotope composition of specific storm samples collected between November 2009 and March 2011. Second, meteorological and streamflow station data were used to examine temporal changes in the contribution of PE precipitation to the annual water budget for each water year from 1960-1995, as well as identify trends in PE storm frequency and magnitude. Finally, relationships between meteorological variables, PE characteristics, and oscillatory climate behaviour were quantified using regression analysis.

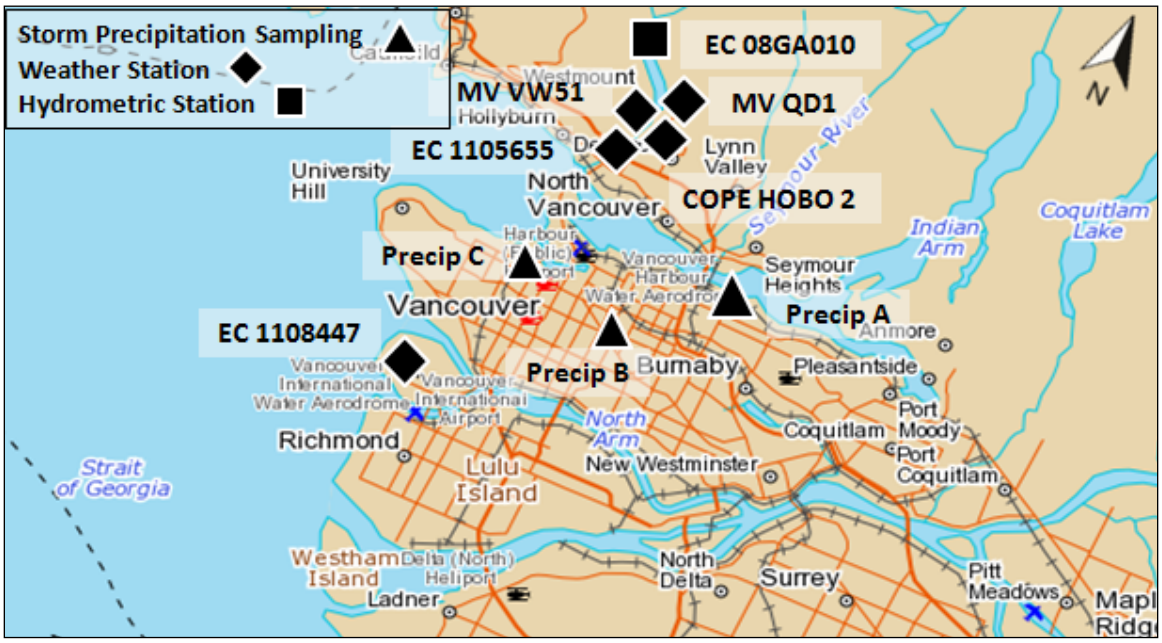

Figure 2.2. Map of the Metro Vancouver area, showing the locations of storm precipitation sampling sites (▲), meteorological stations (♦), and hydrometric stations (■) listed in Table 2.1. Map image retrieved from the digital Atlas of Canada maps (Natural Resources Canada). The map is a reproduction of an official work published by Natural Resources Canada and has not been produced in affiliation with, or with the endorsement of, Natural Resources Canada.

Table 2.1. Site information for all meteorological and hydrometric stations used in this study, and locations where storm precipitation samples were collected for isotopic analysis.

Station Name	Station ID*	Measured Parameters**	Latitude	Longitude	Elevation	Start	End	Application
Vancouver International Airport 1937-Present	EC 1108447	T, P, p, u	49°11'42"N	123°10'55"W	4 m	1948	2007	Frequency and annual storm maxima of PE storms
						1948	2011	Trends in Vancouver climate
						1960	1995	% PE precipitation
						1998	2007	Storm characteristics
Capilano Golf and Country Club 1994-2009	MV VW51	P	49°21'13"N	123°07'29"W	219 m	2005	2007	Storm characteristics
Capilano Water-shed 2005-2011	MV QD1	T, u	49°21'53"N	123°06'16"W	202 m	2005	2007	Storm characteristics
Capilano River Above Intake 1958-Present	EC 08GA010	v	49°23'46" N	123°08'45" W	151 m	1965	1985	% PE stream discharge
						2005	2007	Storm characteristics
North Vancouver Capilano 1955-1990	EC 1105655	P	49°21'00" N	123°07'00" W	93 m	1965	1985	% PE precipitation
Capilano Lake 2010-2012	COPE HOBO-2	T, P, u	49°21'37" N	123°06'22" W	171 m	2010	2011	Characteristics of storms sampled for isotopes
North Burnaby 2009-2010	Precip A	$\delta^{18}O$	49°16'56" N	123°00'20" W	83 m	2009	2010	Collection of storm precipitation samples for oxygen isotope analysis
East Vancouver 2010	Precip B	$\delta^{18}O$	49°15'17" N	123°02'03" W	59 m	2010	2011	Collection of storm precipitation samples for oxygen isotope analysis
Kitsilano 2011	Precip C	$\delta^{18}O$	49°16'13" N	123°09'47" W	38 m	2011	2011	Collection of storm precipitation samples for oxygen isotope analysis

*EC = Environment Canada, MV= Metro Vancouver, COPE= Climate, Oceans and Paleoenvironments Laboratory.

** T= temperature (°C), P= precipitation (mm), p= atmospheric pressure (kPa), u= wind speed (m/s), v= streamflow (m/s), $\delta^{18}O$= oxygen isotope composition (‰).

2.2.1. Meteorological and Streamflow Variables

Meteorological characteristics of PE and non-PE storms were examined by compiling data from all storm events (>20 mm) occurring over a ten year period (1998-2007) at the Vancouver International Airport (Table 2.1; Figure 2.2). The time period of 1998 to 2007 was chosen to allow for comparison with an existing chronology of PE storms identified by Dettinger (2008). A 20 mm per 24-hour period threshold was selected arbitrarily because it represents a precipitation amount that is large enough to be considered an actual storm event, and is likely to have implications for water resource management. Once all storm days were identified based on this precipitation threshold, the total storm precipitation (P) and other corresponding meteorological variables (T, p and u) were also recorded for that day.

In the Capilano region, data from two proximal Metro Vancouver meteorological stations, the Capilano Watershed and Capilano Golf and Country Club, were used (Table 2.1; Figure 2.2). However, data were only available from 2005-2007, and not all variables were available at each station. As a result, P values from the Capilano Golf and Country Club station were used, and variables T and u were taken from the nearby Capilano Watershed station (Table 2.1; Figure 2.2). Neither Capilano station recorded atmospheric pressure. Day-of average streamflow, day-after average streamflow, and two-day total stream discharge were also included, using measurements from the Capilano River Above Intake hydrometric station (Table 2.1, Figure 2.2).

2.2.2. Characterizing PE from non-PE storms

To identify and isolate PE from non-PE storms, each > 20 mm storm day was compared to a chronology of PE events that made landfall between 32.5 and 52.5 °N (Dettinger 2008). Storm days occurring on the day of, immediately before, or immediately after a Dettinger PE event were categorized as PE storms, as they were considered to have occurred due to presence of a PE storm system in the area.

After estimating meteorological and streamflow variables for PE and non-PE storms at both sites, a Mann Whitney test for unpaired data was used to identify which variables, if any, were statistically distinct between the two storm types. Mann-Whitney (aka Rank Sum) is a non-parametric test used to compare the medians of two

independent samples, with the null hypothesis that the “X” (PE storm) and “Y” (non-PE storm) populations are identical (Mann and Whitney, 1947; Swinscow and Campbell, 2002). If the sum of the ranks of each population are statistically different ($p < 0.05$), the null hypothesis is rejected, meaning that PE storms differ significantly from other types of storms in terms of their daily meteorological (precipitation, mean temperature, atmospheric pressure, wind speed) and/or hydrological (day-of average streamflow, day-after average streamflow and 2-day total stream discharge) conditions. A Mann-Whitney test was performed for all variables using the entire data set and then repeated using only the upper quartile of the data. Considering only the upper quartile of hydroclimatic variables allows for comparison of only the highest magnitude storm events, which are of greatest interest from a management perspective.

2.2.3. Isotopic analysis of storm precipitation

In order to characterize the oxygen isotope signature of PE storms making landfall in Metro Vancouver, precipitation samples were collected from 27 storms occurring between November 2009 and March 2011 (see Figure 2.2 for sampling locations). Precipitation samples were collected using a plastic funnel and collection bucket that was set outside during the precipitation event. The apparatus is a modified version of the sampling protocol outlined by the International Atomic Energy Agency (IAEA, 1997) and was used to reduce potential changes in the isotopic ratio of the water sample from evaporation. All storm precipitation samples were filtered using a 0.45μm filter and kept frozen until they were ready for oxygen isotopic ratio analysis at the University of Saskatchewan Isotope Laboratory. A meteorological station was set up in the Capilano Watershed (HOBO-2; Figure 2.2) in February, 2010, to log temperature, precipitation and wind speed of the sampled storm events.

Since the Dettinger (2008) PE chronology ends in 2007, GOES-West satellite imagery (Environment Canada, 2012) was used to classify the isotopic storm samples as PE or non-PE. A PE storm was identified when a winter storm showed evidence of a continuous atmospheric river from around Hawaii to the west coast of North America (Figure 2.1a), thus indicating a subtropical moisture source. Satellite images from the days prior to each sampled storm event were reviewed to verify the AR trajectory of each storm. Storms that did not meet PE criteria were listed as non-PE storms.

Descriptive statistics (i.e., mean, maximum, minimum, standard deviation) and an unbalanced t-test were used to compare the isotopic signature of PE and non-PE storms.

2.2.4. Contribution of PE storms to annual precipitation and stream discharge

The percent contribution of PE storms to the annual water budget in Metro Vancouver was estimated by comparing the cumulative daily PE precipitation and stream discharge at nearby stations to the annual totals for each "water year," 1960-1995. Precipitation data were taken from the Vancouver International Airport and the North Vancouver Capilano weather stations, and stream discharge was calculated from Capilano River Above Intake station daily average streamflow measurements (Table 2.1; Figure 2.2). A water year (WY; October- September) was used instead of calendar year because it allows for comparison to previous analyses of PE storms (Dettinger et al., 2011). The time period (1960-1995) was selected to allow maximum overlap between data sets, as a long and continuous precipitation record for Capilano is only available from 1965-1985. As before, precipitation and stream discharge that occurred on the day of, the day preceding, or the day after a catalogued Dettinger PE storm was considered to be a result of a PE storm system and was included in the total for each water year. The contribution of PE storms to annual precipitation and stream discharge was reported as a percentage value for each water year and plotted as a time series.

2.2.5. Temporal trends in PE frequency and annual storm maxima

Precipitation records from the Vancouver International Airport were used to examine patterns in the frequency (# PE storm days/year) and annual storm maxima (maximum daily precipitation for the largest PE storm in a given year, in mm/day) of PE storms occurring between 1948 and 2007 (Dettinger, 2008). The North Vancouver Capilano time series was not included in this analysis due to the lack of continuous, long-term data. Only storms making landfall between 47.5 and 52.5 °N (Dettinger, 2008) were considered for this analysis, so as to include only storms with direct implications for water resource management in Metro Vancouver. Additionally, because only a small geographical subset of all PE storms was considered, the precipitation threshold of a

"storm event" was set at >10 mm/day for this analysis. Meteorological data from the Vancouver International Airport were also used to identify historical trends in average annual temperature and total annual precipitation, and to consider the influence of climate change on storm patterns in the region. Finally, relationships between annual average temperature, total annual precipitation, annual PE frequency, annual PE storm maxima, and annual average PE water vapour transport rate (estimated from Dettinger, 2008) were quantified using Pearson's r coefficient. The non-parametric Spearman's rank correlation coefficient was also calculated because of its ability to represent non-linear monotonic relationships.

2.2.6. Relationships to climate oscillations

Several previous studies have demonstrated a strong influence of climate oscillations on climate variability along the western North American coast (e.g., Sobel and Maloney, 2000, Miles et al., 2000, Abeysirigunawardena, 2010, Thorne and Woo, 2011, Enloe et al., 2004, Wang et al., 2005). Thus, oscillatory climate behaviour might also influence short-term changes in PE storm behaviour (eg. frequency, annual storm maxima, and % PE contribution to total annual precipitation).

In particular, the Pacific Decadal Oscillation (PDO), the El Niño Southern Oscillation (ENSO) and the Madden-Julian Oscillation (MJO) were chosen for this study because their relationships to PE storms in other regions outside of BC have already been established (e.g., Dettinger, 2004; Jones et al., 2004). The PDO is a multi-decadal oscillation in sea surface temperatures (SSTs), with the positive phase representing a deepening of the Aleutian Low and an intensified SST gradient between the cool western and warm eastern Pacific (Mantua et al., 1997). ENSO is a shorter-period oscillation (~3-7 years) with high SST and atmospheric pressure anomalies occurring during the warm El Niño phase in the eastern tropical Pacific (Trenberth, 1997). The MJO is an intra-seasonal oscillation (~20-90 days) resulting in regions of enhanced and suppressed tropical precipitation, which is most active during the North American winter (Madden and Julian, 1994; Mo, 2011). The MJO is considered to be the dominant mode of intraseasonal variability in the equatorial tropics (Jones et al., 2004). The positive phase of the MJO is associated with enhanced convection in the Indian Ocean, and during the negative phase, the convective region is displaced into the western Pacific

Ocean (Carrasco, 2006). The spatial patterns of the MJO tend to propagate eastward over time.

The relationships between annual oscillatory climate behaviour (PDO, ENSO and MJO) and the frequency and annual storm maxima of PE storms at the Vancouver International Airport (1960-1995) were measured using Pearson and Spearman's rank correlation tests. The PDO Index (Zhang et al., 1997; Mantua et al., 1997) is defined as the primary component of SST variability in the Pacific Ocean, poleward of 20°N (Joint Institute for the Study of Atmosphere and Ocean (JISAO), 2012). The ENSO 3.4 Index refers SST anomalies in the El Niño 3.4 Region, which is bound by 120°W-170°W and 5°S- 5°N (Trenberth, 1997; University Corporation for Atmosphere Research (UCAR), 2012). Data for the MJO Index are only available from 1979 onwards and are based on principal component analysis of the band pass filtered 30-day 850 hPa zonal wind of the equatorial (5ºN – 5ºS) (Maloney and Kiehl, 2002; NOAA, 2003). For all three indices, mean values from October 1-September 30 each year were also calculated, in order to measure Pearson's r and Spearman's ρ for the different climate oscillations and the percentage of PE contribution to total annual precipitation for each water year (1960-1995).

2.3. Results

2.3.1. Characteristics of PE storms

From January 1998 to December 2007, the Vancouver International Airport meteorological station recorded a total of 112 days with > 20 mm precipitation (Appendix). Of those 112 storm days, 32 are considered PE storms (~29%) based on the Dettinger (2008) PE storm chronology. At the Capilano site, a total of 94 storm days with >20 mm precipitation were recorded between 2005 and 2007, 21 of which are considered PE events (~22%; Appendix). A higher number of storm days with > 20 mm precipitation were identified in the Capilano watershed than Vancouver International Airport, likely due to local orographic enhancement of precipitation.

2.3.2. Meteorological and streamflow characteristics

When considering the full datasets of storms, no statistically significant differences are found between PE and non-PE storm variables at Vancouver International Airport, and only three variables at the Capilano site (precipitation, day-after streamflow, and 2-day total stream discharge) demonstrated statistically significant differences (Table 2.2). At the Capilano site, PE storms are associated with higher precipitation than non-PE storms ($p< 0.01$), with PE storms producing an average of 45.6 mm/day compared to non-PE storms with an average of 28.2 mm/day. All discharge variables (day-of average streamflow, day-after average streamflow, and 2-day total stream discharge) are higher for PE storms than non-PE storms in Capilano, but only differences between day-after average streamflow and 2-day total stream discharge are statistically significant ($p<0.05$).

In contrast, a comparison of the upper quartiles (i.e., 75^{th} percentile) at Vancouver International Airport indicate that the highest magnitude PE storms have significantly higher precipitation ($p <0.01$) and lower atmospheric pressure ($p<0.05$) than the largest non-PE storms. In Capilano, high magnitude PE storms were also associated with significantly higher precipitation (75^{th} percentile = 72.2 mm) than the high magnitude non-PE storms (75th percentile = 38.4 mm; $p<0.01$). Furthermore, differences between all streamflow variables for PE and non-PE storms were found to be statistically significant ($p<0.01$; Table 2.2).

Table 2.2. Comparison of meteorological and streamflow characteristics of PE and non-PE storms at two sites in Metro Vancouver, and resulting p-values from Mann-Whitney U tests. N is sample size. Significant values are shown in bold.

Site	Variable	Median			75th Percentile		
		PE Storm	Non-PE Storm	p-Value	PE Storm	Non-PE Storm	p-Value
Vancouver Airport		N=32	N=80		N=8	N=20	
	Temperature (°C)	8.95	7.70	0.0647	11.28	10.20	0.2120
	Precipitation (mm)	27.60	25.50	0.0626	**40.35**	**31.65**	**0.0023**
	Wind speed (m/s)	20.90	19.65	0.0855	25.56	22.76	0.1149
	Atmospheric pressure (kPa)	100.93	100.87	0.6536	**101.35**	**101.55**	**0.0193**
Capilano Watershed		N=21	N=73		N=6	N=19	
	Temperature (°C)	5.03	5.13	0.1692	7.42	7.85	0.0563
	Precipitation (mm)	**45.60**	**28.20**	**0.0025**	**72.20**	**38.40**	**0.0023**
	Wind speed (m/s)	18.88	15.70	0.2631	20.17	19.00	0.1814
	Day-of streamflow (m/s)	28.50	22.60	0.1982	**80.20**	**31.00**	**0.0012**
	Day-after streamflow (m/s)	**160.00**	**42.10**	**0.0006**	**171.00**	**70.20**	**0.0008**
	2-day total stream discharge (m^3/s)	**1357200.00**	**465840.00**	**0.0008**	**1815840.00**	**728640.00**	**0.0009**

2.3.3. $\delta^{18}O$ composition of storm precipitation

Of the 27 storm days sampled for isotopic analysis from November 2009 to March 2011, three were classified as PE storms based on their atmospheric river form and moisture source. The $\delta^{18}O$ composition of the PE storm samples (N=3) ranged from -5.53 to -6.88‰ V-SMOW, with a mean value of -6.10‰ V-SMOW. In contrast, non-PE storm samples (N=24) ranged from -17.66 to -8.5‰, with a mean value of -11.63‰ V-SMOW (Table 2.3). The $\delta^{18}O$ composition of PE storm precipitation making landfall in Vancouver is enriched in ^{18}O relative by an average of 5.5‰ when compared to non-PE storms. In other words, PE precipitation is isotopically heavier. Results from the unbalanced t-test indicate that this difference is significant ($p<0.01$).

Table 2.3. Oxygen isotope composition and meteorological characteristics of PE and non-PE storm precipitation in Metro Vancouver. N/A is not available.

Date	Sampling Location	$\delta^{18}O$ (‰ VSMOW)	Temperature* (°C)	Precipitation* (mm)	Wind Speed* (m/s)
Non-PE storms					
11/02/2010	Precip A	-9.94	N/A	N/A	N/A
26/02/2010	Precip A	-11.48	6.89	12.0	2.57
29/03/2010	Precip A	-9.89	5.19	22.8	1.55
01/04/2010	Precip A	-9.97	4.04	9.8	1.48
30/04/2010	Precip A	-9.00	8.70	2.4	0.76
19/05/2010	Precip A	-9.62	12.18	9.0	1.28
31/08/2010	Precip A	-11.18	11.49	42.2	0.66
08/10/2010	Precip B	-8.50	12.78	6.2	0.61
09/10/2010	Precip B	-8.78	13.83	42.4	0.70
24/10/2010	Precip B	-14.10	9.02	33.0	1.42
18/11/2010	Precip B	-12.55	1.75	9.2	0.23
29/11/2010	Precip B	-10.97	2.04	10.6	0.85
30/11/2010	Precip B	-13.18	2.65	45.6	0.87
08/12/2010	Precip B	-11.86	6.44	49.0	0.45
05/01/2011	Precip B	-12.40	1.32	33.8	1.11
15/01/2011	Precip B	-14.56	6.09	11.4	0.46
24/01/2011	Precip B	-12.83	4.90	33.0	0.69

Date	Sampling Location	$\delta^{18}O$ (‰ VSMOW)	Temperature* (°C)	Precipitation* (mm)	Wind Speed* (m/s)
28/01/2011	Precip B	-9.14	4.56	17.4	1.09
12/02/2011	Precip B	-11.74	4.78	25.2	0.82
14/02/2011	Precip B	-12.17	5.21	39.8	1.59
01/03/2011	Precip C	-13.68	1.01	3.4	0.74
08/03/2011	Precip C	-10.39	2.43	4.0	0.57
13/03/2011	Precip C	-13.50	6.53	13.6	1.72
21/03/2011	Precip C	-17.66	4.62	7.6	0.66
PE storms[b]					
16/11/2009	Precip A	-5.53	N/A	N/A	N/A
15/11/2010	Precip B	-5.89	7.38	27.2	0.16
16/01/2011	Precip B	-6.88	5.17	21.6	0.03

[a] *N*=24, *M*ean $\delta^{18}O$= -11.63‰, *SD* $\delta^{18}O$= 2.19

[b] *N*=3, *Mean* $\delta^{18}O$= -6.10‰, *SD* $\delta^{18}O$= 0.70

* Meteorological characteristics logged by COPE HOBO-2 weather station in the Capilano Watershed, North Vancouver. COPE HOBO-2 was set up on February 19, 2010 and therefore did not record parameters for the first two sampled storm events. Data from a nearby station were not included because of elevation differences and the presence of variable microclimates in the North Shore Mountains.

2.3.4 Contribution of PE storms to total annual precipitation and stream discharge

The contribution of PE storms to the annual water budget is highly variable from year to year and ranges from 0% (during weak PE seasons) to as much as 17% of the total annual precipitation at the Vancouver Airport (WY 1960-1995) and the Capilano watershed (WY 1965-1985; Figure 2.3). Even though the Capilano watershed has higher average annual precipitation than the Vancouver Airport station (2044 mm compared to 1199 mm), the percent contributions of PE precipitation to the annual totals are similar. The mean percent contribution to annual precipitation at the Vancouver Airport and Capilano are 11.0% and 11.9%, respectively. The input of PE storms to total stream discharge over the water year (1965-1985) averages 16.5% for the Capilano watershed, with a maximum contribution of >37% (Figure 2.3). The percentage contribution of PE storms to streamflow is generally higher than its fraction of overall precipitation. However, the two data sets are very well correlated over time.

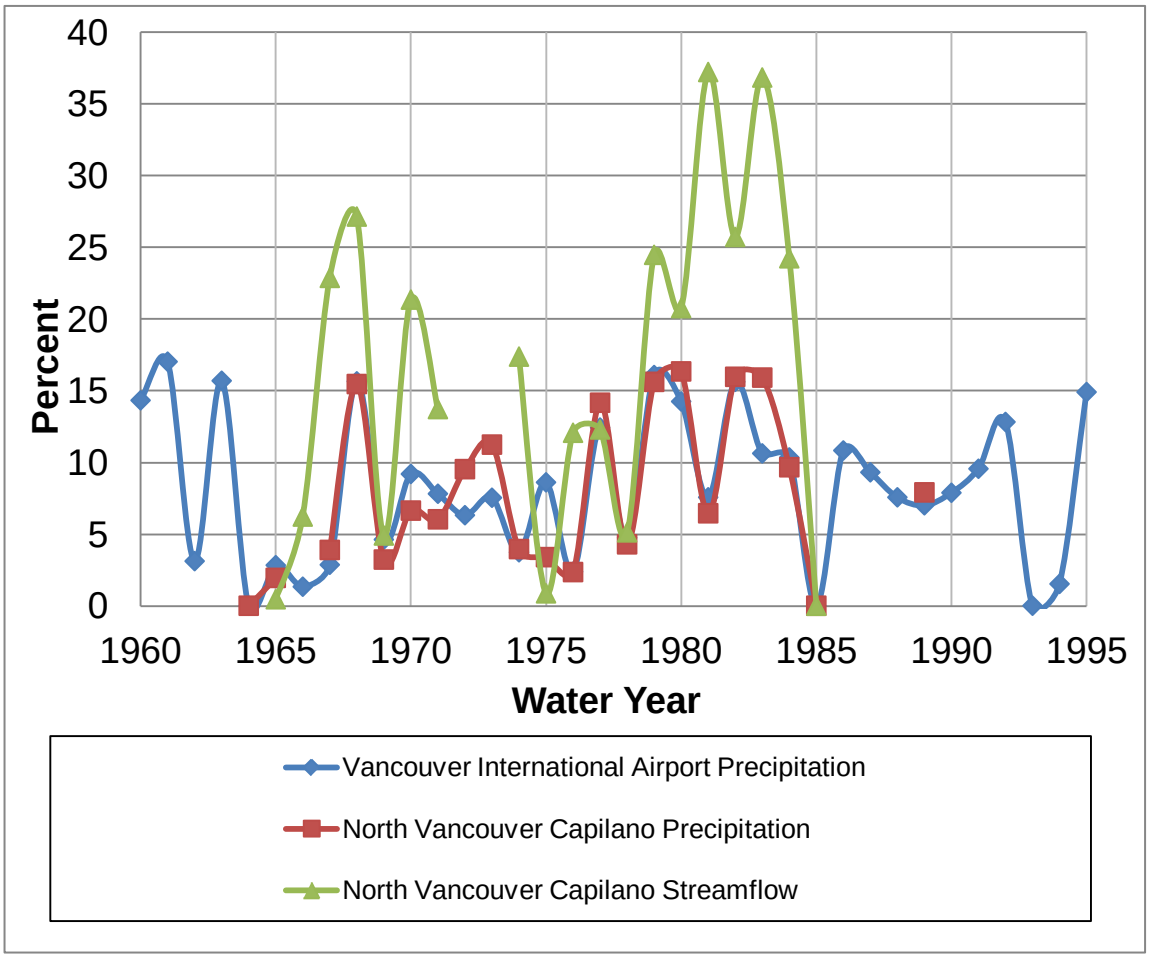

Figure 2.3. Comparison of the percent contribution of PE storms to total annual precipitation and streamflow at two locations in Metro Vancouver, for water years 1960-1995. A "water year" is a 12 month period spanning October 1st-September 30th each year.

2.3.5. Frequency and annual storm maxima of PE storms

At the Vancouver International Airport, a total of 90 days between January 1948 and December 2007 were identified as PE storms using the Dettinger chronology (Dettinger, 2008) and a precipitation threshold of >10 mm/day. The annual frequency of PE storms shows large multi-decadal and interannual variability, with a range of 0-7 PE storm days/year (mean= 1.5 days/ year). The number of distinct storm events is lower, as an individual storm may be represented in the dataset over a period of one to four days (Dettinger, 2008). The largest PE storm maxima recorded at the Vancouver International Airport occurred on January 18, 1968, with 68.3 mm of precipitation in 24

hours. In comparison, most PE storms making landfall in the Vancouver area are <30 mm/day (Figure 2.4). Although no statistically significant trends are observed in PE storm frequency between 1948 and 2007, consistently high frequencies have been observed in recent years (2003-2007; Figure 2.4).

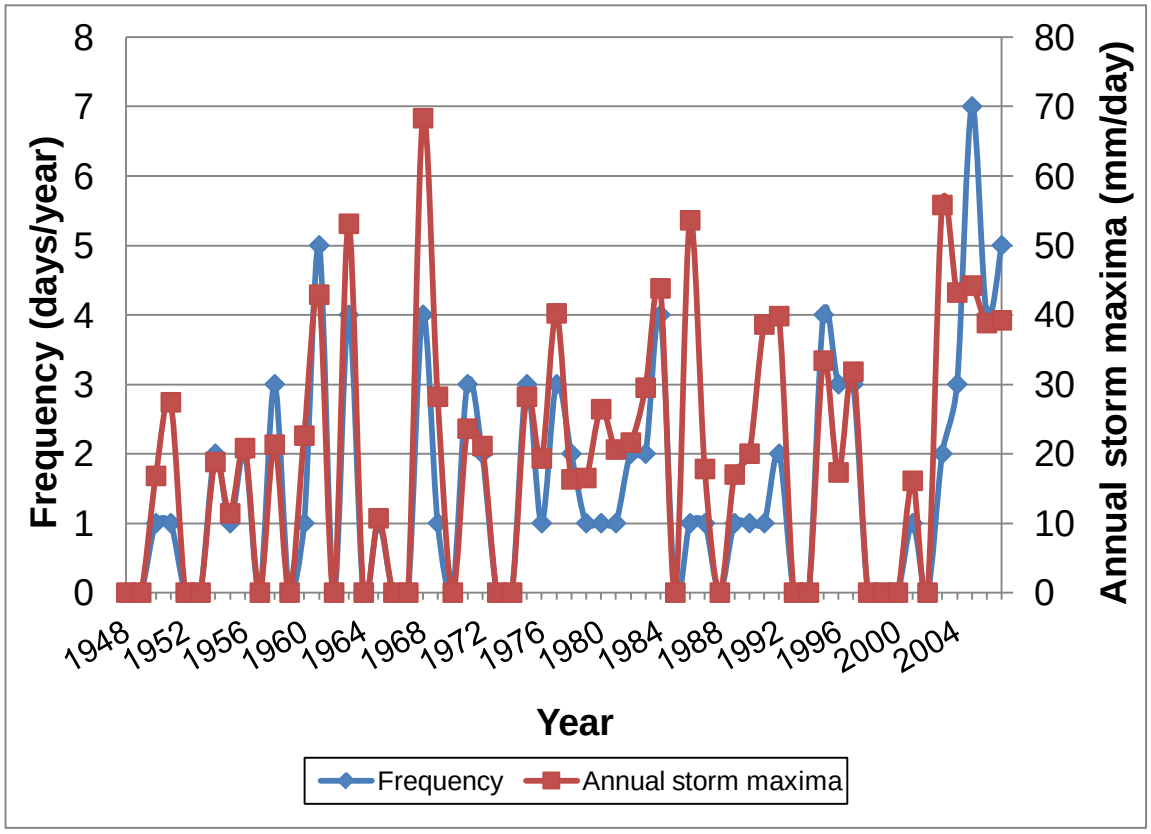

Figure 2.4. PE frequency and annual storm maxima in Metro Vancouver (47.5-52.5°N), 1948-2007. Frequency is displayed as the number of PE storm days/year identified by Dettinger (2008) and PE storm maxima as the total precipitation measured at the Vancouver International Airport for the largest PE storm day in a given year (mm/day).

From 1948-2007, annual average temperature and total precipitation at the Vancouver International Airport showed an overall increasing trend (Figure 2.5). Temperature increased by more than 1°C over this time period, at an average rate of ~0.02°C/year. Precipitation increased by an average of ~2.5 mm/year over the same time period, but also demonstrated high inter-annual variability (standard deviation= 178.67 mm). Results of the linear regression analysis indicate that annual PE storm maxima (i.e., total precipitation for the largest PE storm day in a given year) are

significantly correlated to average temperature (r=0.26, p<0.05), total annual precipitation (r=0.39, p<0.01), annual PE frequency (r=0.79, p<0.01) and annual average vapour transport rate (r=0.46, p<0.01). PE frequency is also significantly correlated with annual water vapour transport rate and total annual precipitation. Analysis using Spearman's ρ indicated similar conclusions, with slightly weakened relationships.

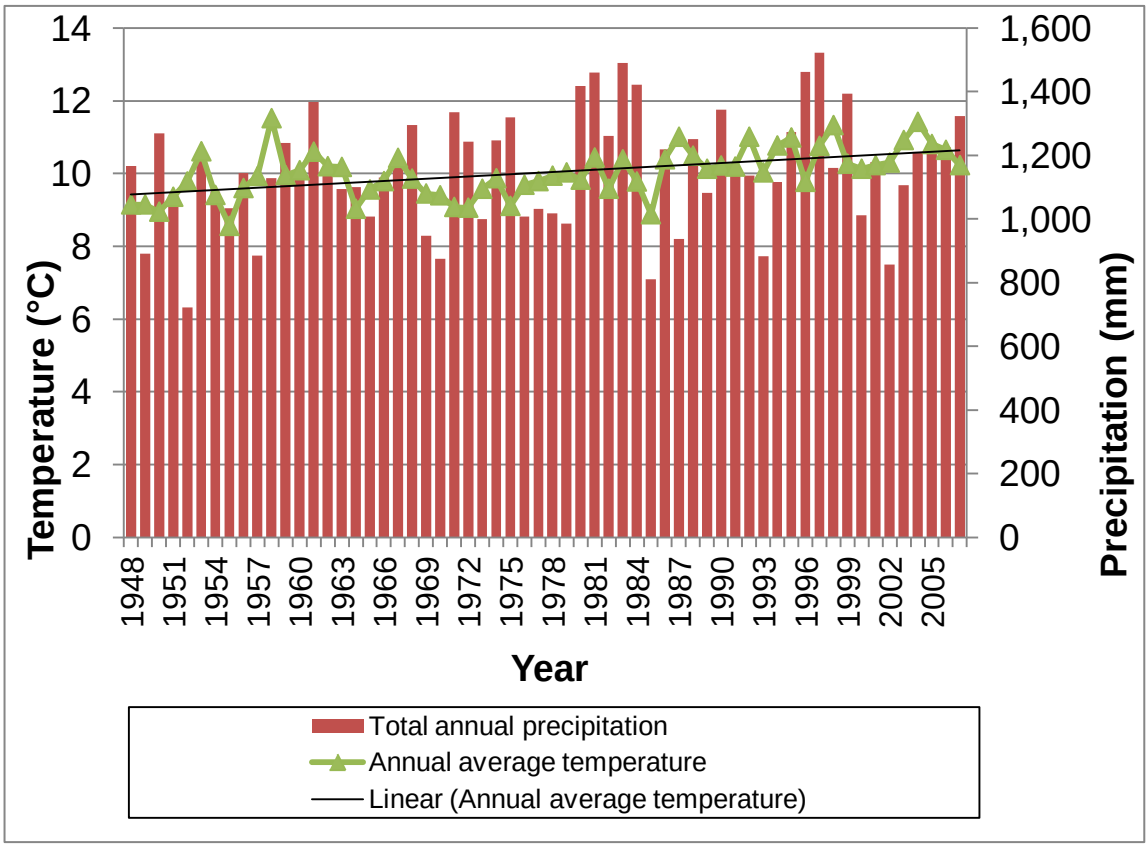

Figure 2.5. Average annual temperature and total annual precipitation at the Vancouver International Airport from 1948-2007. Average annual temperature was calculated from monthly averages, and demonstrates an increasing trend of 0.02°C/year.

2.3.6. Correlation with climate oscillations

The percentage of PE precipitation for the water year exhibits a strong, statistically significant, negative correlation to the mean values for the MJO estimated from October 1-September 30 (ρ= -0.59; p<0.05; Figure 2.6). The MJO index for the calendar year is also correlated with annual PE frequency and annual storm maxima, with the relationship to frequency also being significant (ρ=0.81, p<0.01; Table 2.4). In contrast, PDO and ENSO indices exhibit no correlation with PE storm frequency, annual

PE maxima, and percent contribution of PE storms to annual precipitation (Table 2.4). Pearson's r also found PE storms to be more strongly correlated to the MJO than the PDO or ENSO indices. However, none of these relationships is statistically significant.

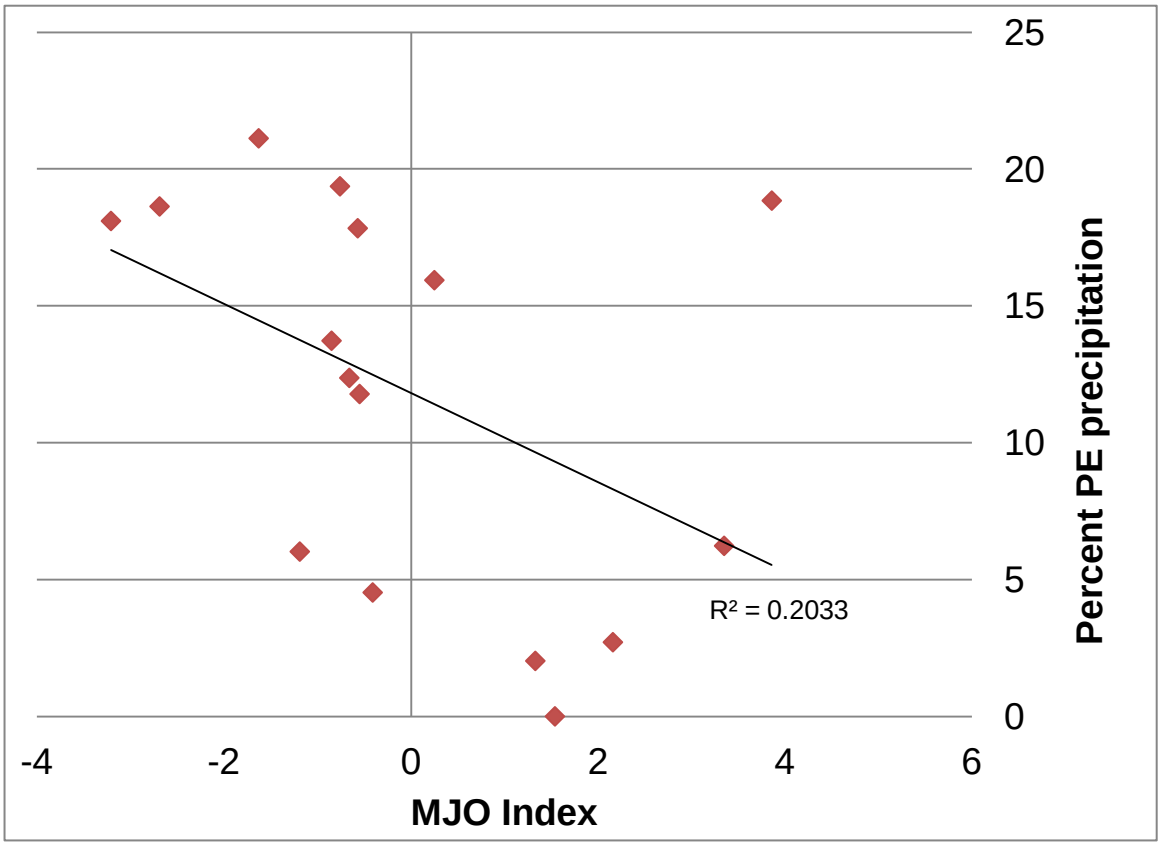

Figure 2.6. Relation between the Madden Julian Oscillation (MJO) and the percent contribution of PE storms to total precipitation at the Vancouver International Airport for water years (October 1-September 30) 1980-1995. The MJO Index shown here is the annual average calculated from daily MJO indices (Maloney and Kiehl, 2002; NOAA 2003).

Table 2.4. Spearman rank correlation coefficients and p values comparing climate indices (PDO, ENSO, and MJO) to PE characteristics (frequency, annual storm maxima and percent contribution to total annual precipitation), 1960-1995. Significant values in bold.

	PDO		ENSO		MJO*	
	ρ	p-value	**ρ**	p-value	**ρ**	p-value
PE Frequency[1]	-0.189	0.268	-0.003	0.985	0.813	<0.001
PE storm maximua[2]	0.006	0.970	0.176	0.305	0.400	0.112
Percent PE precipitation[3]	0.078	0.657	0.105	0.549	-0.588	0.021

[1]# of PE storm days/calendar year
[2] largest PE storm by precipitation to occur in a given calendar year, in mm/day
[3] contribution to total precipitation in a given water year, October- September
*MJO Index only available after 1979.

2.4. Discussion

2.4.1. Distinguishing characteristics of PE storms

Results of the Mann-Whitney test reveal that PE storms are distinguishable from non-PE storms using precipitation and stream discharge variables at both sites in Metro Vancouver, especially when considering only the most extreme (i.e., top quartile) storm events. In fact, the average 75th percentile of PE precipitation in Capilano is nearly double that for precipitation derived from non-PE storms. Similarly, because of the stream response to large inputs of precipitation, the day-of, day-after, and 2-day total stream discharge in the Capilano River are also higher with a PE storm. Comparing the 75th percentiles reveals that 2-day total stream discharge is nearly 250% greater for PE events than non-PE events. Dettinger (2004) also found PE storms produced higher precipitation and streamflow than non-PE storms. In fact, PE storms in the Sierra Nevada yield about twice as much precipitation, and streamflows on the Merced River in Yosemite National Park are approximately an order of magnitude higher following a PE event than other winter storms.

This study demonstrates that PE storms identified via overall morphological characteristics on satellite imagery consistently deliver precipitation with greater $\delta^{18}O$

composition than non-PE storms. The 5.5‰ difference can be attributed to different sources of storm precipitation. Whereas PE storms have a subtropical source (Dettinger, 2004; Dettinger et al., 2011; Ralph and Dettinger, 2011; Mo, 2011), other storms affecting Metro Vancouver originate in the cooler northern Pacific Ocean (Stewart et al., 1995). The spatial variability in isotopic composition of global precipitation is largely temperature dependent, and warm air masses tend to hold moisture that is isotopically heavier than air masses in cooler regions (Dansgaard, 1964; Rozanski et al., 1992). Since PE storm moisture is derived from a tropical to subtropical moisture source, condensation of atmospheric moisture occurs at relatively warmer temperatures than condensation processes occurring in the high-latitude North Pacific where non-PE storms originate.

The oxygen isotope measurements from the Vancouver precipitation samples are consistent with measurements from previous studies conducted in California (Oster et al., 2012; Berkelhammer and Stott, 2008). Oster et al. (2012) sampled two PE storms in the early spring and found them to be isotopically enriched in ^{18}O compared to other early spring precipitation events. Similarly, Berkelhammer and Stott (2008) found that the stable isotope composition of winter PE storms making landfall in northern California were enriched in ^{18}O relative to ^{16}O by approximately 7‰ on average. PE storms in northern California are isotopically heavier (-2.83‰ V-SMOW; Berkelhammer and Stott, 2008) than PE storms making landfall in Metro Vancouver (-6.10‰ V-SMOW), which speaks again to the thermodynamic nature of stable isotope fractionation in the natural environment.

2.4.2. Contribution of PE storms to total annual precipitation and stream discharge

Considering that PE storms only appear a few times each year, they have disproportionately large effects on Vancouver's water resources. Estimates from the Vancouver International Airport and Capilano Watershed demonstrate that PE storms have contributed an average of 11% and a maximum of 17% to total annual precipitation. Therefore, up to nearly one fifth of the city's annual precipitation can theoretically result from the arrival of a single storm. Interestingly, the relative contribution of PE storms was similar at both sites, despite the fact that the North

Vancouver Capilano station receives an average of 70% more precipitation each year than the Vancouver International Airport (based on 1971-2000 climate normals). These results are consistent with Dettinger et al. (2011), who found that PE storms making landfall between Washington and California contributed up to 25% to total annual precipitation from WY 1951-2008. The largest contributions are found in northern California, with values generally decreasing further north and further inland. In Bellingham, Washington, the closest station to Metro Vancouver, the PE contribution to total annual precipitation averaged 15% between WY 1951 and 2008 (Dettinger et al., 2011).

The annual contribution of PE storms to total stream discharge is even higher than that of precipitation (16.5% on average, with a maximum of 37%). The enhanced contribution from PE storms is likely due to PE storms behaving as “rain-on-snow” events. Warm, subtropical PE rain melts existing snowpack on the ground, which runs off into surface water bodies causing a disproportionately high streamflow response (Dettinger, 2004). Again, results are consistent with Dettinger et al. (2011) who also found PE contribution to streamflow to be higher than the contribution to total annual precipitation. In mid-California from WY 1949 to 2008, approximately 55% of annual stream discharge can be attributed to PE events. Percent contributions generally decrease northward and hydrological stations in northwest Washington average around 15% annual PE contribution over the same time period (Dettinger et al., 2011).

2.4.3. Trends in PE storm behaviour

Pineapple Express storms make landfall in and around the Vancouver area (47.5-52.2°N) between 1-2 days/year on average, with a maximum of 7 PE storms days/year between 1948 and 2007. For comparison, PE storms occur approximately 4 days/year across the entire west coast of North America from 32.5-52.2°N (Dettinger, 2004). The actual number of storm events is lower than this because many PEs are multi-day events. Although no statistically significant trend in storm frequency is evident across the entire record, five consecutive years with >2 PE storm days/year have occurred between 2003 and 2007. A five-year period with a consistently high number of annual PE storm days has not occurred previously in the record.

Since the Dettinger (2008) record is only complete through 2007, it is unclear whether or not these trends continued into the future (ie. 2008-2012). If the chronology was brought up to date, it might be possible to test the hypothesis that there is a trend towards a higher number of PE storm days/year. Dettinger (2004) found evidence of an overall increasing trend in the annual frequency of PE circulations in western North America from 1948-1999 (0.18, p=0.2); however, his results were accompanied by a word of caution: the NCEP reanalysis data used to establish the trend were considered less reliable prior to 1979 due to a lack of comparable satellite imagery (Dettinger, 2004; Bylhouwer et al., 2013).

The years 2005-2007 exhibited a similar unprecedented trend of three consecutive years with annual storm day maxima of approximately 40 mm or more. The largest recorded historical PE storm day at the Vancouver International Airport was on January 19, 1968, with 68.5 mm of precipitation. On the same day, the North Vancouver Capilano station recorded 89.2 mm of precipitation. The positive correlations between PE annual storm maxima with PE frequency and total annual precipitation (1948-2007) suggest that strong Pineapple Express years can bring numerous high magnitude storm events over a single season. Linear regression also indicates a statistically significant positive correlation between the PE storm day maxima and annual average temperature. Since warmer years tend to be associated with the highest magnitude PE storms, rising global temperatures can potentially lead to significant damages and costs to society resulting from increased PE storm activity.

The annual average temperature at the Vancouver Airport increased at a rate of 0.02°C/year from 1948-2007 (Figure 2.5). If temperatures continue to rise at the linear historical rate, then the annual average temperature could approach 11.5°C by 2050, which represents a 2.5°C increase from average temperatures in 1950 (8.95°C). This type of linear temperature projection based on historical temperature behaviour may be somewhat simplistic, but nevertheless is consistent with regional projections from climate model simulations. For comparison, the Intergovernmental Panel on Climate Change (IPCC) AR4 global climate model projections suggest that by the 2050s, annual temperatures in British Columbia are estimated to be +1.7°C (+1.2°C to +2.5°C) warmer than the 1961 – 1990 baseline, and the Canadian Regional Climate Model (CRCM4) estimates a +2.6°C (+2.0°C to +3.0°C) warming over the same time period (Rodenhuis

et al., 2009). Thus, it might be anticipated that these warmer years in the future could result in greater PE storm day maxima than typically seen in the past.

2.4.4. Relationships with climate oscillations

El Niño years bring warmer temperature and less precipitation to BC than their La Niña counterparts, while positive (warm) PDO years tend to have variable effects on precipitation, and negative (cool) PDO years tend to be associated with wetter conditions (Fleming et al., 2006; Stahl et al., 2006; Wang et al., 2006). However, in this study, the PDO and ENSO indices show no direct correlation to PE storm characteristics (frequency, annual storm day maxima and contribution to annual precipitation) over the interval of 1960 to 1995 (Table 2.4). These results are supported by Dettinger (2004) who also found no correlation between the frequency and magnitude of PE storms with ENSO. Nonetheless, Dettinger (2004) did note that every El Niño season from 1948-2004 had a minimum of one PE event, whereas >50% of La Niña seasons had no PE storms. The strongest PE seasons have occurred during neutral ENSO years, in phase with a positive PDO, when the westerlies are further south and have greater access to warm, subtropical moisture (Mantua et al., 1997). As the PDO is a multi-decadal oscillation, the time series from the Vancouver International Airport used in this study may be too short to resolve low frequency climate variability.

The relationships between PE characteristics and the MJO are much stronger than those with the PDO or ENSO, especially when using Spearman's ρ because the relationships are monotonic. The MJO exerts a strong negative correlation to the percent contribution of PE storms to total precipitation and a strong positive correlation to PE frequency (Vancouver International Airport, WY1980-1995). Both correlations are significant. When the MJO is in a negative phase, enhanced convection occurs in the western equatorial Pacific Ocean, which can fuel Pineapple Express storms and thus lead to a higher contribution of PE storm precipitation to annual totals. These results are similar to other studies which found mean daily and monthly precipitation amounts during the negative phase of the MJO to be significantly higher than during the positive phase (Carrasco, 2006; Nazemosadat and GHaed Amini Asad Abadi, 2009). The MJO is believed to exert a strong influence on the PE storms because the tropical temperature anomalies associated with the MJO allow for the development of the characteristic 500-

hPa geopotential height anomalies of PE events (Mo, 2011; Lackmann and Gyakum, 1999). This mid-tropospheric pressure pattern allows low pressure cyclones to develop along cold fronts, which drive warm, subtropical air to the west coast of North America along a persistent storm track (Ralph et al*.,* 2004; Neiman et al., 2008a). On rare occasions, heavy tropical rainfall from the MJO in the Indian Ocean can feed tropical moisture directly into the PE system as it shifts eastwards. This phenomenon creates the most severe type of PE storm, coined as a "tropical punch" by meteorologists (Mo, 2011).

The long time scale of the ENSO and PDO oscillations (multi-annual and multi-decadal) means that they may be influencing overall seasonal hydroclimatic (precipitation and streamflow) characteristics with limited impact on individual extreme storm events that occur only 1-2 days/year in southwest BC. The MJO is a much shorter term oscillation (20-90 days) that is more closely related to atmospheric dynamics that can influence individual, extreme storm behaviour resulting from rapid atmospheric vapour transport. The strong correlation between PE storms and the MJO supports the notion that the MJO is considered to be the dominant mode of intraseasonal variability in the equatorial tropics (Jones et al., 2004).

2.4.5. Relationship between PE storms, water resources and natural hazards in BC

The distinctive hydroclimatic characteristics of PE storms translate into real socioeconomic risks that must be managed accordingly. The intense precipitation and rapid streamflow of PE storms in the Metro Vancouver area highlight two major causes for concern: impacts to municipal water resources (supply and quality) and the increased potential for precipitation-induced natural hazards.

PE storms play a dichotomous role for regional water supply in the Lower Mainland of British Columbia. The powerful storms can lead to excess runoff and flooding hazards during the winter season, but also store valuable water resources as snowpack at higher elevations, which is essential for maintaining adequate supply during dry summer periods (Environment Canada, 2004). PE storms in Metro Vancouver can contribute up to 17% of the total annual precipitation, and thus the occurrence of one or

two major PE storms over a winter season might make the difference between a particularly wet year and a summer drought. Future demand-side management protocols may need to be considered as population growth places increased pressure on water resources, and climate change contributes to summer drought conditions (Metro Vancouver, 2011b; ACT, 2011).

PE storms may contribute to decreased water quality by triggering geomorphic processes that result in elevated turbidity levels into drinking water reservoirs and drinking water intakes (Jakob and Weatherly, 2003; Metro Vancouver, 2011b; Vancouver Sun, 2006). In Metro Vancouver, the Capilano Reservoir is particularly vulnerable to turbid water episodes due to intense and prolonged rainstorms it receives, particularly in the fall-winter period, combined with the steep terrain, local hydrology, soil moisture conditions, and surficial material characteristics (Armstrong, 1990). Slope failures, bank erosion, and gullying, particularly on fine-grained glaciolacustrine deposits, can give the drinking water a cloudy appearance if it reaches the drinking water intake. If turbidity levels are unacceptably elevated at the intake, the water supply from the Capilano source is not distributed to the municipalities as alternative water supplies from the two other Metro Vancouver drinking water sources are available (City of Vancouver, 2011). It is anticipated that Capilano, like the Seymour source in 2009, will be filtrated some time in 2014.

The highest recorded turbidity values are typically associated with the initiation of a slope failure such as debris flows and/or gully erosion in the watershed. For example, in November 2006, a series of Pineapple Express storms triggered debris slides and flows and other forms of erosion across the North Shore Mountains where Metro Vancouver's water supply originates. Antecedent precipitation enhances soil moisture, and thus is a leading factor in landslide initiation in the North Shore Mountains (Jakob and Weatherly, 2003). Turbidity levels at both the Capilano and Seymour sources exceeded 50 NTU for a period of time (Greater Vancouver Regional District, 2007). The recommended level for tap water is 1 NTU, and 5 NTUs triggers an advisory from the local medical health authorities. Because of operational constraints neither source could be removed from service. As a result, a "boil water advisory" was issued as a precautionary health measure for the entire system on November 16. The area affected by the advisory was reduced the next day to the North Shore municipalities, Vancouver,

Burnaby, and the Point Grey/UBC area. The advisory remained in effect for another 10 days, and is considered to be one of the largest in Canadian history (Vancouver Sun, 2006; Natural Resources Canada, 2009).

PE storms can also decrease water quality through nonpoint and point source pollution. Stormwater can contain motor oil, gasoline, sediment, fertilizer and other contaminants of concern (Metro Vancouver, 2011c) or lead to sanitary sewer overflows (SSOs) during periods of heavy rainfall (Metro Vancouver, 2011c; Hall et al*.,* 1991; Hall and Macdonald, 1996). Of the upmost concern are combined sewer outflows (CSOs), a legacy of the region's original sewerage system that allows wastewater and storm water run through the same pipe. Combined sewers are being replaced by separate sanitary and storm sewers, but the high cost of infrastructure replacement creates a barrier to storm water mitigation (Metro Vancouver, 2010).

In some cases, the occurrence of high magnitude PE storms may pose a direct threat to public safety resulting from natural hazards. For this study, a comparison of the 382 storm days identified by Dettinger (2008) with records of flooding, avalanches, debris flows and avalanches in northern BC (Septer, 2007) shows that 74 of those days (19.4%) correspond with a natural hazard. Flooding was the most frequently observed natural hazard, coinciding with 60% of all PE storms (N=37) between 1950 and 2006. Snow avalanches and landslides/debris flows occurred with 41% and 24% of all PE storms. The arrival of PE storms also corresponds with debris flows affecting residents near Chilliwack, BC. Of 18 debris flows reported between 1980 and 2007 in the Hatzic Valley and the Bridal Falls Corridor near Chilliwack, 11 (61%) correspond to a PE storm making landfall between 45 and 52.5°N (Sutton, 2011). PE storms tend to have higher precipitation rates than other storm types and occur during the rain-on-snow season, which could lead to enhanced association between debris flows and PE storms.

2.4.6. Planning for future PE events

The societal vulnerability to impacts from PE storms can be expected to increase as climate continues to warm and influence storm behaviour as is evidenced by the positive relationship between annual PE storm maxima with frequency and average annual temperature. Also, a multi-model analysis by Dettinger (2011) suggests that

under the A2 emissions scenario (with rapid acceleration of greenhouse gas emissions) we can expect little change in the annual frequency of December-February AR days, but years with many AR storms will become more frequent, as will the number of ARs with higher-than-historical water vapour transport rates. Municipal and provincial climate change adaptation policies for extreme weather events in the Metro Vancouver need to account for these projected changes in PE storm patterns occurring at the extremes.

The Vancouver Climate Change Adaptation Strategy (City of Vancouver, 2012) outlines plans to minimize the risks to society from future increases in the intensity and frequency of heavy rain events. Plans include the design and implementation of a citywide integrated stormwater management plan by 2014. The city aims to decrease the total amount of impermeable surfaces to reduce flood risks, and to divert stormwater runoff from the sewer system through the separation of sanitary and stormwater sewers (to be completed by 2050; City of Vancouver, 2012; Metro Vancouver, 2008). Other efforts to improve water quality include the reduction of nonpoint source pollution in the Burrard Inlet through the introduction of stormwater Best Management Practices (BMPs) for local waterfront businesses (BIEAP, 2010), and the construction of a new drinking water treatment facility in the Lower Seymour Conservation Reserve (Metro Vancouver, 2011b). The treatment facility already serves the Seymour water source and is expected to be online for the Capilano water source by 2014, once the twin tunnels that connect Capilano to the Seymour Conservation Reserve Filtration Plant are completed (Metro Vancouver, 2011d).

Municipal strategies receive support from the Province of British Columbia, who committed $95 million in 2008 to climate change adaptation research and policy development, and handles issues related to public, emergency preparedness and disaster relief (British Columbia Ministry of Environment, 2010; Henstra and McBean, 2009; EMBC, 2012). Municipal and provincial strategies discuss risk management as considering both the severity and probability of impacts, but fail to include a range of potential risk scenarios that would account for the inter- and intra-annual variability of winter storm patterns on British Columbia's southwest coast. More emphasis should be placed on addressing how specific adaptation measures would measure up against even the rarest and most severe type of PE storm: a PE superstorm. Wet weather sewer overflows can occur with storms having return periods of 1:2 or 1:5 (Metro Vancouver,

2010), so extremely large storm events drastically increase the potential for overflows and other negative impacts.

The largest storm event in California in recent history was a PE superstorm over the winter of 1861-1862, an event so large it has a historical reoccurrence rate of 150-400 years (Porter et al., 2011). The storm produced record precipitation, extensive flooding, and hundreds of landslides that contributed to a death toll in the thousands. The population of California has increased a hundred-fold since then, and the reoccurrence of an event this size could result in hundreds of billions of dollars in damages (Porter et al., 2011). Since PE storms can occur across the entire latitudinal range of western North America, it is reasonable to assume that a superstorm of this magnitude could one day impact British Columbians by making landfall along the southern coast of BC. At-risk municipalities on British Columbia's south coast could follow California's lead, as they have begun planning for "ARkStorm": a hypothetical Pineapple Express superstorm scenario modelled after the storm event of 1861-1862. The goal of the ARkStorm is to map out the socioeconomic impacts of a PE superstorm across the State of California in order to identify and remediate vulnerabilities (Porter et al., 2011). Vancouver could adapt ARkStorm conditions to the environment and socioeconomic specific to their own city, and demonstrate how they have prepared for even the worst case scenario.

2.5. Conclusions

Pineapple Express (PE) storms are warm, wet and intense AR storms that have not previously been well documented or characterized in Vancouver, BC. By identifying storms using an independent chronology of PE events (Dettinger, 2008), this study shows that PE storms bring statistically higher precipitation to multiple regions in Vancouver and result in statistically larger streamflows, particularly when considering the subset of more extreme (75^{th} percentile) storms. PE storms are also distinguishable by the isotopic composition of their precipitation, which is made up of heavier oxygen isotopes than storm types that originate at higher latitudes in the Pacific Ocean. An analysis of meteorological records from 1948 to 2007 suggests that Vancouver has historically experienced anywhere from 0-7 PE storm days/year, which contribute an

average of 11% and 17% to annual precipitation and stream discharge totals. Both the PE frequency (# storm days/year) and annual storm day maxima (mm precipitation/day) exhibit high interannual variability without any long-term trends, although both variables seem to be on the rise in recent years.

The frequency and magnitude of Pineapple Express circulations are also influenced by their response to climate oscillations and a warming climate. Results indicate that the percent contribution of PE precipitation to total annual precipitation is strongly negatively correlated to the Madden-Julian Oscillation (MJO) Index. In other words, water years with higher percentages of PE rain tend to occur with during negative phases of the MJO, when convection in the western equatorial Pacific Ocean is enhanced. MJO tropical precipitation anomalies serve as a moisture source for the subtropical PE system, and fuel the high magnitude AR storms witnessed on the west coast of North America as the MJO propagates eastward. Additionally, the annual PE storm maxima are positively correlated to annual average temperatures. Since PE storms in Metro Vancouver have been linked to water supply, water quality, and precipitation-induced natural hazards, a warmer climate could result in a higher occurrence of high magnitude PE storms capable of costly damages and risks to public safety.

This work has focused on identifying PE characteristics and trends for Metro Vancouver, but future work should focus on assessing long-term trends. Longer time series would help to identify controlling factors by including more PE storms in the analysis, as they occur less than two days/year on average. Extending the record of PE events can also be achieved by maintaining an up-to-date chronology of PE events in future. Using the criteria outlined by Dettinger (2004), the Dettinger (2008) PE record can be extended using large-scale reanalysis data. Results could be supplemented by continued isotopic sampling of storm precipitation and using satellite imagery to further distinguish storm trajectories and moisture sources. A more rigorous storm precipitation sampling methodology performed over a longer time frame would allow for further investigation into controls over the isotopic composition of precipitation, and has the potential to distinguish between true PE storms, near misses, and the most intense “Tropical Punch” PE storms that can originate in the eastern Indian Ocean. From a policy perspective, it is recommended that the City of Vancouver consider the potential

environmental and socioeconomic impacts that could result from a superstorm scenario. The city has drafted a climate change adaptation strategy (City of Vancouver, 2012), but more emphasis should be placed on addressing the low probability but extremely high magnitude storm events on the scale of the PE superstorm that decimated California over the winter of 1861-1862.

2.6. References

Abeysirigunawardena, D.S. 2010. Climate variability and change impacts on coastal environmental variables in British Columbia Canada. British Columbia: University of Victoria, PhD thesis, 322 pp.

Adaptation to Climate change Team (ACT). 2011. *Background report: Climate change adaptation and water governance*. Vancouver, British Columbia: Simon Fraser University, 130 pp.

Armstrong, J. E. 1990. *Vancouver Geology*. Vancouver, British Columbia: The Geological Association of Canada, 130 pp.

Berkelhammer, M. B. and L. D. Stott. 2008. Recent and dramatic changes in Pacific storm trajectories recorded in $\delta^{18}O$ from Bristlecone Pine tree ring cellulose. *Geochemistry, Geophysics, Geosystems* 9:Q04008.

British Columbia Ministry of Environment. 2010. *Preparing for Climate Change: British Columbia's Adaptation Strategy*. British Columbia: Government of British Columbia, 8 pp.

Burns, S.F., W. J. Burns, D. H. James, and J. C. Hinkle. 1998. Landslides in Portland, Oregon metropolitan area resulting from the storm of February 1996: Inventory map, database, and evaluation. Portland, Oregon: METRO.

Burrard Inlet Environmental Action Program (BIEAP). 2010. *Who knows where the stormwater goes? A pilot project to promote stormwater Best Management Practices in Vancouver*. Vancouver, British Columbia: Burrard Inlet Environmental Action Program, 49 pp.

Bylhouwer, B., D. Ianson, and K. Kohfeld. 2013. Changes in the onset and intensity of wind-driven upwelling and downwelling along the North American Pacific Coast. *Journal of Geophysical Research – Oceans* 118:1–16.

California Department of Water Resources (CDWR). 2002. *Final Recommendations Report*. Sacramento, California: California Flood Management Task Force, 29 pp.

Carrasco, J. F. 2006. Precipitation events in central Chile and its relation with the MJO. In *Proceedings of the Eighth International Conference on Southern Hemisphere Meteorology and Oceanography,* Foz de Iguacu, Brazil: American Meteorological Society, 1719-1722.

City of Vancouver. 2011. Drinking water quality 2010 annual report. Vancouver, British Columbia: City of Vancouver, 52 pp.

City of Vancouver. 2012. *Climate change adaptation strategy*. Vancouver, British Columbia: The Sustainability Group, 74 pp.

Dansgaard, W. 1964. Isotopes in precipitation. *Tellus* 16:4.

Dettinger, M. 2004. *Fifty-two years of "Pineapple-Express" storms across the west coast of North America.* California: United States Geological Survey, Scripps Institutions of Oceanography for the California Energy Commission, PIER Energy-Related Environmental Research, CEC-500-2005-004.

Dettinger, M. 2005. A long-term (~50-yr) historical perspective on flood-generating winter storms in the American River basin. In *Proceedings of the California Extreme Precipitation Symposium*. Sacramento, California, April 22, 2005.

Dettinger, M. 2008. Pineapple Express Record 1948-2007. Unpublished Data.

Dettinger, M.D. 2011. Climate change, atmospheric rivers, and floods in California- A multi-model analysis of storm frequency and magnitude changes. *Journal of the American Water Resources Association* 47(3):514-523.

Dettinger, M. D., F. M. Ralph, T. Das, P. J. Neiman, and D. R. Cayan. 2011. Atmospheric rivers, floods and the water resources of California. *Water* 3:445-478.

Emergency Management British Columbia (EMBC). 2006a. *Flooding Situation Overview: November 6, 2006 21:00 Hrs.* http://www.pep.bc.ca/hazard_preparedness/flooding_Nov_2006/ Nov_6 -06_210 0hrs.pdf (Accessed April 2012).

EMBC. 2006b. *Flooding Situation Overview: November 7, 2006 16:00 Hrs.* http://www.pep.bc.ca/hazard_preparedness/flooding_Nov_2006/Nov_7-06_1600hrs.pdf (Accessed April 2012).

EMBC, 2012. *All-Hazard Plan*. British Columbia: Emergency Management British Columbia, 64 pp.

Enloe, J., J. O'Brien, and S. Smith. 2004. ENSO Impacts on Peak Wind Gusts in the United States. *Journal of Climate* 17(8): 1728-1737.

Environment Canada. 2004. Threats to water availability in Canada, NWRI Scientific Assessment Report Series No. 3 and ACSD Science Assessment Series No. 1. Burlington, Ontario: National Water Research Institute, 128 pp.

Environment Canada. 2012. *Weather Office*. http://www.weatheroffice.gc.ca/canada_e.html (Accessed March 2012).

Fleming, S., R. D. Moore, and G. K. C. Clarke. 2006. Glacier-mediated streamflow teleconnections to the Arctic Oscillation. *International Journal of Climatology* 26: 619–636.

Greater Vancouver Regional District. 2007. The Greater Vancouver water district quality control annual report 2007: Volume 2 Chemical and Physical Monitoring Results. Vancouver, British Columbia: The Greater Vancouver Regional District, 166 pp.

Hall, K. J., H. Schreier and S. J. Brown. 1991. Water quality in the Fraser River Basin. In *Water in sustainable development: Exploring our common future in the Fraser River Basin*, ed. A. H. J. Dorcey and J. R. Griggs, 41-75. Vancouver, British Columbia: Westwater Research Centre, The University of British Columbia.

Hall, K. J. and R. H. Macdonald. 1996. Water *quality and stormwater in the Brunette River Watershed: Water sampling program 1994/1995: Data Report and Appendices.* Vancouver, British Columbia: Westwater Research Unit, Institute of Resources and Environment, The University of British Columbia.

Henstra, D. And G. McBean. 2009. *Climate change and extreme weather: Designing Adaptation Policy*. British Columbia: Adaptation to Climate Change Team, 47 pp.

International Atomic Energy Agency (IAEA). 1997. *Technical procedure for sampling.* http://www-naweb.iaea.org/napc/ih/documents/userupdate/sampling.pdf (Accessed September, 2011).

Jakob, M. and H. Weatherly. 2003. A hydroclimatic threshold for landslide initiation on the North Shore mountains of Vancouver, British Columbia. *Geomorphology* 54(3-4):137-156.

Jakob, M. and S. Lambert. 2009. Climate change effects on landslides along the southwest coast of British Columbia. *Geomorphology* 107(3-4): 275-284.

Joint Institute for the Study of the Atmosphere and Ocean. 2012. *PDO Index*. http://jisao.washington.edu/pdo/PDO.latest (Accessed February, 2012).

Jones, C., D. E. Waliser, K. M. Lau, and W. Stern. 2004. Global occurrences of extreme precipitation and the Madden-Julian Oscillation: Observations and predictability. *Journal of Climate* 17: 4575-4589.

Junker, N. W., R. H. Grumm, R. Hart, L. F. Bosart, K. M. Bell, and F. J. Pereira. 2008. Use of normalized anomaly fields to anticipate extreme rainfall in the mountains of northern California. *Weather Forecasting* 23: 336-356.

Lackmann, G. M. and J. R. Gyakum. 1999. Heavy cold-season precipitation in the northwestern United States: Synoptic climatology and an analysis of the flood of 17–18 January 1986. *Weather and Forecasting* 14(5): 687-700.

Madden, R. A., and P. R. Julian. 1994. Observations of the 40–50-day tropical oscillation: A review. *Monthly Weather Review* 122: 814–837.

Maloney, E. D. and J. T. Kiehl. 2002. MJO-related SST variations over the tropical eastern Pacific during Northern Hemisphere summer. *Journal of Climate* 15: 675-689.

Mann, H. B. and D. R. Whitney. 1947. On a test of whether one of two random variables is stochastically larger than the other*. Journal of Statistical Computing and Simulation* 13: 41–48.

Mantua, N. J., S. R. Hare, Y. Zhang, J. M. Wallace, and R. C. Francis. 1997. A Pacific interdecadal climate oscillation with impacts on salmon production. *Bulletin of the American Meteorological Society* 78: 1069-1079.

Metro Vancouver. 2008. *Vulnerability of Vancouver sewerage infrastructure to climate change.* Burnaby, British Columbia: Metro Vancouver, 94 pp.

Metro Vancouver. 2010. Integrated liquid waste and resource management: A liquid waste management plan for the Greater Vancouver Sewerage & Drainage District and member municipalise. Burnaby, British Columbia Metro Vancouver, 38 pp.

Metro Vancouver. 2011a. *Sources & supply*. http://www.metrovancouver.org/services/water/source/Pages/default.aspx (Accessed April 2013).

Metro Vancouver. 2011b. *Drinking water management plan.* Burnaby, British Columbia: Metro Vancouver Sustainable Region Initiative, 22 pp.

Metro Vancouver. 2011c. *Stormwater management*. http://www.metrovancouver.org/services/wastewater/sources/Pages/StormwaterManagement.aspx (Accessed April 2012).

Metro Vancouver. 2011d. *Seymour-Capilano Water Utility Projects.* http://www.metrovancouver.org/services/constructionprojects/water/Pages/seymourcapilano.aspx (Accessed March 2013).

Miles, E. L., A. Hamlet, A. K. Snover, B. Callahan and D. Fluharty. 2000. Pacific Northwest regional assessment: The impacts of climate variability and climate change on the water resources of the Columbia River Basin. *Journal of American Water Resources Association* 36(2): 399-420.

Mo, R. 2011. Pineapple Express. In *Meteorology today: An introduction to weather, climate and the environment*, ed. C. D. Ahrens, P. L. Jackson, and C. E. O. Jackson, 375. Connecticut: Cengage Learning.

Natural Resources Canada. 2009. *How do the cycles and modes of the Pacific Ocean affect the water cycle?* http://www.nrcan.gc.ca/earth-sciences/climate-change/landscape-ecosystem/by-theme/3213 (Accessed June 2012).

Nazemosadat, S., H. GHaed Amini AsadAbadi. 2009. The influence of Madden-Julian Oscillation on occurrence of February to April Extreme Precipitation (Flood and Drought) in Fars Province. *Journal of Science and Technology of Agriculture and Natural Resources, Water and Soil Science* 12(46): 477-489.

Neiman, P. J., F. M. Ralph, A. B. White, D. E. Kingsmill, and P. O. G. Persson. 2002. The statistical relationship between upslope flow and rainfall in California's Coastal Mountains: Observations during CALJET. *Monthly Weather Review* 130: 1468-1492.

Neiman, P. J., F. M. Ralph, G. A. Wick, Y. Kuo, T. Wee, Z. Ma, G. H. Taylor, and M. D. Dettinger. 2008a. Diagnosis of an intense atmospheric river impacting the Pacific Northwest: Storm summary and offshore vertical structure observed with COSMIS Satellite Retrievals. *Monthly Weather Review* 136(11): 4398-4420.

Neiman, P. J., F. M. Ralph, G. A. Wick, J. Lundquist, and M. D. Dettinger. 2008b. Meteorological characteristics and overland precipitation impacts of atmospheric rivers affecting the West Coast of North America based on eight years of SSM/I satellite observations. *Journal of Hydrometeorology* 9(1): 22– 47.

National Oceanic and Atmospheric Association (NOAA). no date. *Notable atmospheric river events.* http://www.esrl.noaa.gov/psd/atmrivers/events/ (Accessed March 2012).

NOAA, 2003. *Monitoring Weather & Climate*. http://www.cpc.ncep.noaa.gov/products/precip/CWlink/daily_mjo_index/pentad.html (Accessed February, 2012).

Oster, J. L., I. P. Montañez and N.P. Kelley. 2012. Response of a modern cave system to large seasonal precipitation variability. *Geochimica et Cosmochimica Acta* 91: 92-108.

Parker, L.E. 2009. Meteorological conditions associated with rain-related periglacial debris flows on Mount Hood, Oregon and Mount Rainier, Washington. Oregon: Oregon State University Master's thesis, 103 pp.

Porter, K., A. Wein, C. Alpers, A. Baez, P. Barnard, J. Carter, A. Corsi, J. Costner, D. Cox, T. Das, M. Dettinger, J. Done, C. Eadie, M. Eymann, J. Ferris, P. Gunturi, M. Hughes, R. Jarrett, L. Johnson, H. Dam Le-Griffin, D Mitchell, S. Morman, P. Neiman, A. Olsen, S. Perry, G. Plumlee, M. Ralph, D. Reynolds, A. Rose, K. Schaefer, J. Serakos, W. Siembieda, J. Stock, D. Strong, I. Sue Wing, A. Tang, P. Thomas, K. Topping, Ken, and C. Wills. 2011. *Overview of the ARkStorm scenario*. Virginia: United States Geological Survey, Open-file report 2010-1312, 183 pp.

Ralph, F. M., P. J. Neiman, and G. A. Wick. 2004. Satellite and CALJET aircraft observations of atmospheric rivers over the eastern North-Pacific Ocean during the winter of 1997/98. *Monthly Weather Review* 132: 1721-1745.

Ralph, F. M., P. J. Neiman, and R. Rotunno. 2005. Dropsonde observations in low-level jets over the northeastern Pacific Ocean from CALJET-1998 and PACJET-2001: Mean vertical-profile and atmospheric-river characteristics. *Monthly Weather Review*, 133(4): 889–910.

Ralph, F. M. and M. D. Dettinger. 2011. Storms, floods and the science of atmospheric rivers. *Eos, Transactions of the American Geophysical Union* 92(32): 265-272.

Rodenhuis, D., K. Bennett, A. Werner, T. Murdock and D. Bronaugh. 2009. *Climate Overview 2007- Hydro-climatology and future climate impacts in British Columbia*. Victoria, British Columbia: Pacific Climate Impacts Consortium, University of Victoria, 132 pp.

Rozanski, K., L. Araguasaraguas and R. Gonfiantini. 1992. Relationship between long-term trends of O-18 isotope composition of precipitation and climate. *Science* 258(5084): 981-985.

Salathé, E. P. 2006. Influences of a shift in North Pacific storm tracks on western North American precipitation under global warming. *Geophysical Research Letters* 33: L19820.

Salathé, E. P., R. Steed, C. F. Mass, and P. H. Zahn. 2008. A high-resolution climate model for the United States Pacific Northwest: Mesoscale feedbacks and local responses to climate change. *Journal of Climate* 21: 5708–5726.

Septer, D. 2007. *Flooding and landslide events northern British Columbia 1820-2006.* British Columbia: Ministry of Environment, 216 pp.

Sobel, A. H., and E. D. Maloney. 2000. Effect of ENSO and the MJO on western north Pacific tropical cycles. *Geophysical Research Letters* 27(12): 1739-1742.

Stahl, K., R. D. Moore, and I. G. McKendry. 2006. The role of synoptic-scale circulation in the linkage between large-scale ocean atmosphere indices and winter surface climate in British Columbia, Canada. *International Journal of Climatology* 26:541–560.

Stewart , R. E., D. Bachand , R. R. Dunkley , A. C. Giles , B. Lawson , L. Legal , S. T. Miller , B. P. Murphy , M. N. Parker , B. J. Paruk, and M. K. Yau. 1995. Winter storms over Canada. *Atmosphere-Ocean* 33(2): 223-247.

Sutton, E. 2011. *Influence of meteorological controls on debris flows near Chilliwack, British Columbia*. Burnaby, British Columbia: Simon Fraser University, School of Resource and Environmental Management, 81 pp.

Swinscow, T. D. V. and M. J. Campbell. 2002. *Statistics at Square One*. London: BMJ Books, BMJ Publishing Group.

Tebaldi C., K. Hayhoe, J. M. Arblaster, and G. A. Meehl. 2006. Going to the extremes: An intercomparison of model-simulated historical and future changes in extreme events. *Climatic Change* 79: 185–211.

Thorne, R., and M. K.Woo. 2011. Streamflow response to climate variability in a complex mountainous environment: Fraser River Basin, British Columbia, Canada. *Hydrological Processes* 25: 3076-3085.

Trenberth, K. E. 1997. The definition of El Niño. *Bulletin of the American Meteorological Society* 78: 2771-2777.

University Corporation for Atmospheric Research. 2012. *TNI (Trans-Niño Index) and N3.4 (Niño 3.4 Index).* http://www.cgd.ucar.edu/cas/catalog/climind/TNI_N34/index.html#Sec5 (Accessed February, 2012).

Vancouver Sun. 2006. *Boil-water advisory may last well into weekend.* http://www.canada.com/vancouversun/news/story.html?id=a889657f-9ea7-4d57-b491-6fbc9ca24359 (Accessed November 2012).

Wang, T., A. Hamann, D. Spittlehouse, and S. N. Aitkens. 2006. Development of scale-free climate data for western Canada for use in resource management. *International Journal of Climatology* 26(3): 383-397.

Wang, X. L., H. Wan and V. R. Swail. 2005. Observed changes in cyclone activity in Canada and their relationships to major circulation regimes. *Journal of Climate* 19: 896-915.

Yin, J. H. 2005. A consistent poleward shift of the storm tracks in simulations of 21st century climate. *Geophysical Research Letters* 32: L18701.

Zhang, Y., J. M. Wallace, D. S. Battisti. 1997. ENSO-like interdecadal variability: 1900-93. *Journal of Climate* 10: 1004-1020.

Zhu, Y., and R. E. Newell. 1998. A proposed algorithm for moisture fluxes from atmospheric rivers. *Monthly Weather Review* 126: 725-735.

2.7. Appendix. Meteorological and streamflow characteristics of all storm days at the Vancouver International Airport (1998-2007; N=112) and the Capilano Watershed (mid 2005-2007; N=94).

Daily mean temperature (T), 24 hour precipitation (P), wind speed (u), atmospheric pressure (p), streamflow (v) and stream discharge (V). A precipitation threshold of 20 mm was used to classify a "storm day". Values are pulled directly from station data, except for 2-day total stream discharge, which was estimated from mean daily streamflow measurements. PE storms accounted for 29% and 22% of all storm days at the Vancouver International Airport and the Capilano Watershed, respectively.

Storm date	PE (0=no, 1=yes)	T (°C)	P (mm)	u (m/s)	p (kPa)	v (day-of, m/s)	v (next-day, m/s)	V (2-day total, m^3)
Vancouver International Airport (Station EC 1108447), 1998-2007.								
14-Jan-98	0	7.1	22.6	23.8	99.8	N/A	N/A	N/A
23-Jan-98	1	8.2	22.2	27.8	100.0	N/A	N/A	N/A
12-Feb-98	0	8.6	20	22.3	100.1	N/A	N/A	N/A
15-May-98	0	11.3	22.6	15.1	101.6	N/A	N/A	N/A
27-May-98	0	10.1	35.2	16.6	101.4	N/A	N/A	N/A
12-Nov-98	1	8.6	27.2	26.3	101.4	N/A	N/A	N/A
14-Nov-98	0	10.2	42.6	22.3	100.9	N/A	N/A	N/A
15-Nov-98	0	12	25.6	28.3	100.1	N/A	N/A	N/A
20-Nov-98	0	9.4	25.4	27.5	99.7	N/A	N/A	N/A
29-Nov-98	0	4.6	21.2	21.3	100.1	N/A	N/A	N/A
05-Dec-98	0	4	25.6	26.0	100.7	N/A	N/A	N/A
12-Dec-98	0	9.5	40.5	29.3	101.1	N/A	N/A	N/A
24-Dec-98	0	0.3	23.7	20.4	101.8	N/A	N/A	N/A
27-Dec-98	1	4.2	28	18.9	100.0	N/A	N/A	N/A
29-Dec-98	1	9	22.2	19.3	101.3	N/A	N/A	N/A
14-Jan-99	0	7.3	32.8	21.0	100.8	N/A	N/A	N/A
28-Jan-99	0	4.3	20.6	22.0	100.7	N/A	N/A	N/A
29-Jan-99	0	6	36.3	26.6	100.3	N/A	N/A	N/A
03-Feb-99	0	4.1	23.6	21.1	100.8	N/A	N/A	N/A
22-Feb-99	0	7.4	22.2	30.2	100.7	N/A	N/A	N/A

Storm date	PE (0=no, 1=yes)	T (°C)	P (mm)	u (m/s)	p (kPa)	v (day-of, m/s)	v (next-day, m/s)	V (2-day total, m^3)
24-Feb-99	0	7.6	25.1	23.3	99.8	N/A	N/A	N/A
02-Jul-99	0	11.8	42.4	10.3	100.9	N/A	N/A	N/A
29-Oct-99	0	8.1	31.8	20.7	102.2	N/A	N/A	N/A
30-Oct-99	0	8.4	48.2	12.5	101.6	N/A	N/A	N/A
06-Nov-99	0	10.1	22	17.1	100.8	N/A	N/A	N/A
11-Nov-99	1	10.8	24	15.0	100.8	N/A	N/A	N/A
01-Dec-99	0	6.2	20.4	22.0	101.3	N/A	N/A	N/A
15-Dec-99	1	8.8	49	22.5	101.1	N/A	N/A	N/A
03-Mar-00	0	7	20.4	15.6	101.8	N/A	N/A	N/A
02-Jul-00	0	13.9	25.8	9.9	101.8	N/A	N/A	N/A
27-Jul-00	0	16	26.2	15.7	101.5	N/A	N/A	N/A
29-Sep-00	1	14.9	23.2	16.8	101.3	N/A	N/A	N/A
16-Oct-00	0	10.2	23	15.8	101.4	N/A	N/A	N/A
20-Oct-00	0	11.7	27.4	27.5	100.3	N/A	N/A	N/A
16-Dec-00	0	2.5	38.5	26.7	101.1	N/A	N/A	N/A
04-Jan-01	0	7.9	34.3	16.8	101.9	N/A	N/A	N/A
01-Mar-01	0	4.5	22.4	17.3	100.6	N/A	N/A	N/A
21-Aug-01	0	15	23.4	21.1	100.9	N/A	N/A	N/A
22-Aug-01	0	15.6	22	15.0	100.8	N/A	N/A	N/A
18-Oct-01	0	9.2	22.3	16.0	102.4	N/A	N/A	N/A
12-Dec-01	0	1.9	22.4	19.6	101.3	N/A	N/A	N/A
13-Dec-01	0	7	38	22.7	99.3	N/A	N/A	N/A
15-Dec-01	0	4.8	36.2	28.7	100.0	N/A	N/A	N/A
06-Feb-02	0	6	23.4	18.3	100.9	N/A	N/A	N/A
21-Feb-02	0	7.2	26.4	17.9	101.5	N/A	N/A	N/A
13-Apr-02	1	12.8	20.2	21.9	100.6	N/A	N/A	N/A
18-Nov-02	0	9.7	25.8	24.7	101.8	N/A	N/A	N/A
19-Nov-02	0	11.8	30.6	17.9	102.4	N/A	N/A	N/A
01-Jan-03	1	5.9	21.6	24.8	101.4	N/A	N/A	N/A
02-Jan-03	1	8.8	23.4	29.8	100.5	N/A	N/A	N/A

Storm date	PE (0=no, 1=yes)	T (°C)	P (mm)	u (m/s)	p (kPa)	v (day-of, m/s)	v (next-day, m/s)	V (2-day total, m^3)
22-Jan-03	1	6	21.8	18.8	101.0	N/A	N/A	N/A
12-Mar-03	0	9	21.7	24.5	99.9	N/A	N/A	N/A
07-Apr-03	0	8.3	28.8	27.1	101.6	N/A	N/A	N/A
24-Apr-03	0	7.4	24.4	9.0	100.8	N/A	N/A	N/A
16-Oct-03	1	11.5	85	26.4	100.5	N/A	N/A	N/A
17-Oct-03	1	15	55.8	18.1	100.8	N/A	N/A	N/A
20-Oct-03	1	15.9	25.4	21.2	100.9	N/A	N/A	N/A
18-Nov-03	0	6.8	37	13.5	100.7	N/A	N/A	N/A
28-Nov-03	0	7.3	62.6	29.3	100.8	N/A	N/A	N/A
07-Jan-04	0	2	22.2	21.7	100.6	N/A	N/A	N/A
29-Jan-04	0	7.1	21.2	15.0	100.4	N/A	N/A	N/A
10-Sep-04	0	15.7	26.4	18.3	101.1	N/A	N/A	N/A
18-Sep-04	0	11.8	91.6	15.5	100.4	N/A	N/A	N/A
08-Oct-04	0	13.1	21	18.0	100.7	N/A	N/A	N/A
17-Oct-04	0	10	22.8	9.0	99.2	N/A	N/A	N/A
01-Nov-04	0	5.7	35	20.6	102.1	N/A	N/A	N/A
06-Nov-04	1	8.2	43.2	15.6	102.0	N/A	N/A	N/A
24-Nov-04	0	10.3	27.6	20.1	101.0	N/A	N/A	N/A
04-Dec-04	0	5.7	35.4	21.9	100.2	N/A	N/A	N/A
10-Dec-04	1	9.5	26.2	22.8	100.9	N/A	N/A	N/A
25-Dec-04	0	5.4	33.4	19.9	100.6	N/A	N/A	N/A
17-Jan-05	1	6.2	56.6	20.0	101.4	N/A	N/A	N/A
18-Jan-05	1	9.9	44.2	15.8	101.6	N/A	N/A	N/A
19-Jan-05	1	12.6	28.4	19.3	101.5	N/A	N/A	N/A
22-Jan-05	1	11.2	39.4	20.6	101.3	N/A	N/A	N/A
04-Feb-05	0	7.4	21.8	19.0	101.3	N/A	N/A	N/A
26-Mar-05	1	8.4	33	29.7	100.7	N/A	N/A	N/A
29-Sep-05	0	14	39.2	17.2	100.9	N/A	N/A	N/A
16-Oct-05	0	11.8	20.2	16.4	101.7	N/A	N/A	N/A
20-Dec-05	1	8.9	23.6	15.1	101.3	N/A	N/A	N/A

Storm date	PE (0=no, 1=yes)	T (°C)	P (mm)	u (m/s)	p (kPa)	v (day-of, m/s)	v (next-day, m/s)	V (2-day total, m^3)
31-Dec-05	0	7.6	22.4	15.7	98.9	N/A	N/A	N/A
09-Jan-06	0	7.3	26.8	20.0	101.0	N/A	N/A	N/A
10-Jan-06	0	6.5	27.6	17.9	99.8	N/A	N/A	N/A
16-Jan-06	0	5.9	29.8	24.9	101.4	N/A	N/A	N/A
29-Jan-06	0	3.8	23.4	20.8	100.7	N/A	N/A	N/A
08-Mar-06	0	4.1	25	31.5	100.5	N/A	N/A	N/A
08-Jun-06	0	14.3	25.8	14.5	101.7	N/A	N/A	N/A
15-Oct-06	0	10.8	31.6	14.5	100.1	N/A	N/A	N/A
03-Nov-06	1	11.2	44.6	19.4	100.3	N/A	N/A	N/A
04-Nov-06	1	12	22.4	25.3	100.7	N/A	N/A	N/A
06-Nov-06	1	13.9	35.8	26.4	100.3	N/A	N/A	N/A
10-Nov-06	0	7.5	30	23.0	100.5	N/A	N/A	N/A
12-Nov-06	0	7.6	24.4	19.7	100.4	N/A	N/A	N/A
15-Nov-06	1	8.8	38.8	42.5	99.6	N/A	N/A	N/A
17-Nov-06	0	7.8	21.2	18.5	101.8	N/A	N/A	N/A
26-Nov-06	0	-0.6	20.6	12.6	99.9	N/A	N/A	N/A
24-Dec-06	1	5.7	24.4	21.5	101.5	N/A	N/A	N/A
02-Jan-07	1	9.3	28.2	25.0	100.4	N/A	N/A	N/A
18-Jan-07	0	2.4	20	18.0	102.7	N/A	N/A	N/A
14-Feb-07	1	6.1	23.2	18.4	102.2	N/A	N/A	N/A
11-Mar-07	1	11.1	39.2	18.2	101.2	N/A	N/A	N/A
17-Mar-07	0	8.7	30.2	13.8	101.5	N/A	N/A	N/A
22-Mar-07	0	5.9	20.4	20.0	101.9	N/A	N/A	N/A
23-Mar-07	0	8.2	23.4	23.9	101.4	N/A	N/A	N/A
24-Jun-07	0	12.4	20.6	11.0	101.6	N/A	N/A	N/A
30-Sep-07	0	10.4	44	25.4	100.6	N/A	N/A	N/A
18-Oct-07	0	8.2	24.4	17.8	100.0	N/A	N/A	N/A
19-Oct-07	0	8.9	27.2	14.1	100.0	N/A	N/A	N/A
21-Oct-07	0	9.2	25.6	19.0	102.6	N/A	N/A	N/A
26-Nov-07	0	2.1	21	14.5	101.6	N/A	N/A	N/A

Storm date	PE (0=no, 1=yes)	T (°C)	P (mm)	u (m/s)	p (kPa)	v (day-of, m/s)	v (next-day, m/s)	V (2-day total, m^3)
02-Dec-07	1	0.1	25.8	16.5	99.8	N/A	N/A	N/A
03-Dec-07	1	7.4	46.4	27.7	99.8	N/A	N/A	N/A
Capilano Watershed (Stations MV VW51, MV QD1, EC 08GA010), 2005-2007.								
16-Jun-05	0	15.2	22.8	19.3	N/A	7.9	10.5	303048
4-Jul-05	0	16.3	34.2	10.9	N/A	4.2	11.1	324576
7-Jul-05	0	15.2	24.2	13.0	N/A	13.3	78.1	267552
28-Sep-05	0	10.1	80.4	16.3	N/A	4.2	55.1	696168
5-Oct-05	0	9.4	31.8	9.7	N/A	6.4	34.9	298872
14-Oct-05	0	10.6	38.8	11.8	N/A	27.8	99.4	363960
15-Oct-05	0	10.3	31.6	9.7	N/A	99.4	42.1	297144
16-Oct-05	0	9.5	23.6	16.4	N/A	42.1	82.5	288144
18-Oct-05	0	10.0	31.4	16.7	N/A	29.2	27.8	346392
29-Oct-05	0	7.0	30.4	10.3	N/A	30.1	68.6	292680
30-Oct-05	0	6.8	23.0	22.1	N/A	68.6	119.0	324576
31-Oct-05	0	8.1	28.0	18.1	N/A	119.0	43.7	331776
2-Nov-05	0	5.1	27.4	15.5	N/A	48.0	54.0	309168
7-Nov-05	0	4.5	21.0	10.0	N/A	18.7	17.8	223200
9-Nov-05	0	4.6	24.0	17.1	N/A	27.6	85.0	295776
19-Dec-05	1	3.2	41.8	5.6	N/A	2.8	89.1	341136
21-Dec-05	1	9.5	21.6	18.9	N/A	134.0	169.0	291456
23-Dec-05	1	7.4	45.6	17.8	N/A	67.0	172.0	456408
30-Dec-05	0	5.1	23.8	15.7	N/A	28.3	53.2	284400
4-Jan-06	0	4.9	33.8	17.8	N/A	22.4	93.3	371448
8-Jan-06	0	4.3	53.8	18.3	N/A	38.2	64.7	519336
9-Jan-06	0	3.9	27.2	20.0	N/A	64.7	47.4	339552
11-Jan-06	0	3.9	23.8	16.2	N/A	31.0	24.1	288072
12-Jan-06	0	3.8	26.4	21.5	N/A	24.1	85.7	345168
15-Jan-06	0	1.7	35.8	11.1	N/A	20.3	19.2	337896
21-Jan-06	0	1.9	25.4	11.2	N/A	12.6	12.6	263304
25-Jan-06	0	4.8	20.0	14.6	N/A	17.8	21.5	249336

Storm date	PE (0=no, 1=yes)	T (°C)	P (mm)	u (m/s)	p (kPa)	v (day-of, m/s)	v (next-day, m/s)	V (2-day total, m^3)
27-Jan-06	0	2.3	20.4	18.1	N/A	18.9	20.3	277056
28-Jan-06	0	3.2	22.2	23.3	N/A	20.3	15.2	327240
30-Jan-06	0	3.8	30.8	11.5	N/A	29.5	19.7	304560
3-Feb-06	0	3.8	22.8	19.8	N/A	20.3	74.4	306648
7-Mar-06	0	4.3	40.8	14.9	N/A	20.3	15.2	401184
21-Mar-06	0	5.0	44.8	19.4	N/A	6.3	55.2	462096
12-Apr-06	0	7.1	24.8	14.7	N/A	19.2	20.8	284184
31-May-06	0	14.2	39.2	10.7	N/A	24.0	52.2	359064
7-Jun-06	0	14.6	43.8	12.8	N/A	23.9	38.8	407160
19-Sep-06	0	11.8	37.0	13.2	N/A	4.5	7.9	361512
14-Oct-06	0	10.1	61.8	11.0	N/A	3.7	3.7	524160
24-Oct-06	0	7.2	25.8	23.5	N/A	2.7	2.8	354960
25-Oct-06	0	5.1	34.2	11.3	N/A	2.8	40.9	327240
1-Nov-06	1	1.9	40.8	5.6	N/A	4.5	8.2	333936
2-Nov-06	1	5.4	68.8	8.4	N/A	8.2	167.0	555696
3-Nov-06	1	9.9	35.6	19.4	N/A	167.0	160.0	396144
4-Nov-06	1	10.9	45.2	25.3	N/A	160.0	82.3	507837.6
5-Nov-06	1	9.4	80.2	15.5	N/A	82.3	200.0	689040
9-Nov-06	0	4.1	51.2	13.2	N/A	14.6	215.0	463464
11-Nov-06	0	3.8	54.0	12.7	N/A	24.0	47.0	480024
14-Nov-06	1	3.1	81.6	20.2	N/A	19.1	215.0	732744
16-Nov-06	1	3.2	31.6	21.3	N/A	71.3	64.7	380520
20-Nov-06	0	5.6	23.2	18.8	N/A	48.0	67.0	302040
3-Dec-06	0	0.3	30.0	5.5	N/A	4.0	7.6	255888
10-Dec-06	0	5.0	24.4	13.5	N/A	36.7	123.0	272592
13-Dec-06	0	5.2	24.6	27.6	N/A	55.3	36.5	376056
23-Dec-06	0	1.5	25.4	11.3	N/A	15.9	21.4	264456
31-Dec-06	1	2.4	86.6	10.3	N/A	6.1	22.2	697896
1-Jan-07	1	2.5	80.2	26.8	N/A	22.2	165.0	770328
4-Jan-07	0	1.0	33.6	25.7	N/A	23.2	17.2	426744

Storm date	PE (0=no, 1=yes)	T (°C)	P (mm)	u (m/s)	p (kPa)	v (day-of, m/s)	v (next-day, m/s)	V (2-day total, m^3)
5-Jan-07	0	0.4	23.6	29.1	N/A	17.2	18.5	379656
6-Jan-07	0	2.1	34.8	24.3	N/A	18.5	19.2	425160
17-Jan-07	0	-0.5	47.4	11.2	N/A	5.3	5.3	421704
18-Jan-07	0	0.2	29.8	18.0	N/A	5.3	8.0	344448
21-Jan-07	1	0.9	50.4	16.6	N/A	5.9	15.0	482256
22-Jan-07	1	1.5	54.8	20.0	N/A	15.0	55.4	538848
13-Feb-07	1	5.2	25.0	7.3	N/A	28.5	25.5	232488
14-Feb-07	1	3.8	25.0	18.4	N/A	25.5	43.8	312336
18-Feb-07	0	5.0	47.2	15.4	N/A	23.3	27.3	450576
9-Mar-07	1	5.0	30.2	18.9	N/A	59.5	80.2	353376
10-Mar-07	1	7.0	73.2	17.7	N/A	80.2	258.0	654264
15-Mar-07	0	2.6	24.0	11.4	N/A	17.2	17.3	255024
16-Mar-07	0	3.2	47.0	10.8	N/A	17.3	45.2	416376
21-Mar-07	0	1.2	40.2	16.0	N/A	27.6	29.9	404928
22-Mar-07	0	2.3	81.8	20.0	N/A	29.9	93.7	732960
23-Mar-07	0	5.8	38.6	23.9	N/A	93.7	165.0	449856
25-Apr-07	0	5.9	28.2	15.0	N/A	28.9	70.2	310752
26-Apr-07	0	7.5	21.6	19.0	N/A	70.2	104.0	292608
1-May-07	0	8.0	29.2	14.5	N/A	18.5	38.4	314640
19-May-07	0	9.1	27.0	15.3	N/A	32.0	50.4	304776
8-Jun-07	0	13.1	25.8	11.5	N/A	22.6	34.7	268560
20-Jul-07	0	14.9	22.6	16.3	N/A	22.2	76.9	280296
29-Sep-07	0	7.7	46.2	24.0	N/A	4.7	183.0	505728
5-Oct-07	0	6.6	22.8	11.3	N/A	15.8	15.9	245736
16-Oct-07	0	7.9	22.8	18.8	N/A	30.2	34.8	299736
17-Oct-07	0	5.5	25.6	18.3	N/A	34.8	50.5	315720
18-Oct-07	0	5.8	38.4	17.8	N/A	50.5	54.9	404568
20-Oct-07	0	5.7	52.6	19.0	N/A	68.8	70.5	515520
21-Oct-07	0	6.7	22.0	19.0	N/A	70.5	102.0	295200
2-Nov-07	0	3.2	30.4	12.3	N/A	7.0	10.9	307656

Storm date	PE (0=no, 1=yes)	T (°C)	P (mm)	u (m/s)	p (kPa)	v (day-of, m/s)	v (next-day, m/s)	V (2-day total, m^3)
11-Nov-07	0	5.9	20.0	25.9	N/A	52.2	111.0	330336
14-Nov-07	0	3.3	25.8	10.8	N/A	19.5	69.0	263160
25-Nov-07	0	1.5	23.0	6.9	N/A	5.7	5.4	215424
1-Dec-07	1	-2.3	26.4	23.8	N/A	3.9	3.9	361656
2-Dec-07	1	-0.1	72.2	16.5	N/A	3.9	206.0	638352
3-Dec-07	1	7.6	22.6	27.7	N/A	206.0	246.0	361944
12-Dec-07	0	0.2	25.8	6.7	N/A	6.2	5.7	234072

Chapter 3.

Regional Climate Patterns Recorded in Tree Ring Isotopes in British Columbia

3.1. Introduction

Tree ring records provide a useful means of examining the characteristics of climate change prior to instrumental records (Li et al., 2011; Briffa et al., 2013), and the oxygen isotope ($\delta^{18}O$) ratio of α-cellulose in tree rings has the potential to provide even further information about regional paleoclimate (McCaroll and Loader, 2004). The relative abundance of oxygen isotopes in precipitation varies with changes in temperature, precipitation, and the source of the moisture and storm trajectory (Dansgaard, 1964; Gat, 1996; Lee and Fung, 2008). Once the precipitation infiltrates the soil, it becomes accessible for uptake by trees, and the isotopic signature of that precipitation can get incorporated into the woody tissues of trees as they grow (McCaroll and Loader, 2004). As a result, the $\delta^{18}O$ values of tree ring cellulose reflect mainly the ^{18}O composition of the source water (precipitation and soil water), though the $\delta^{18}O$ values can also be influenced by biophysical factors such as leaf evaporative enrichment, xylem water sucrose and biosynthesis (Sternbern, 2009; Anderson et al., 2002). Such local biophysical effects, however, are considered to be similar for individual trees of the same species grown in the same environment, so they are assumed to be insignificant (Anderson et al., 2002; Miller et al., 2006). Thus, analysis of inter- and intra-annual changes in oxygen isotope ratios in tree rings has the potential to provide a high-resolution historical record of past climatic conditions.

The study of oxygen isotopes in tree ring α-cellulose has been shown to be an effective tool for reconstructing paleoclimate in several different geographic regions (Bale et al., 2010; Shu et al., 2005; Berkelhammer and Stott, 2008; Porter, 2009;

Brienen et al., 2012; Saurer et al., 2012), and in some cases has even provided a record of seasonal storm activity (Miller et al., 2006; Sano et al., 2012). For example, Miller et al. (2006) developed a 220-year $\delta^{18}O$ tree ring record from a Longleaf Pine near Valdosta, Georgia, as a proxy record for tropical cyclone occurrence along the Atlantic seaboard. Intense precipitation events are typically more depleted in ^{18}O because of the "precipitation amount effect", wherein precipitation from a storm cloud becomes increasingly depleted in ^{18}O along its trajectory because of the preferential condensation of heavy oxygen isotopes (Gat, 1996; Lee and Fung, 2008; Jouzel et al., 2003). In this case, Miller et al. (2006) found that the most depleted ^{18}O values in the latewood cellulose tended to correspond to known cyclone events within the historical records.

In the Pacific Northwest region of North America, storms originating in the subpolar region of the North Pacific Ocean have isotopic signatures that are as much 5-6‰ more depleted in ^{18}O than tropical and subtropical systems like the Pineapple Express (Berkelhammer and Stott, 2008; Chapter 2). This large isotopic difference between storm sources raises the possibility that tree ring isotope records might also incorporate some climate-related changes in the dominant source of precipitation from Pacific storms that reach the coast. However, unlike the intense summer storms seen along the east coast of the United States, the west coast of North America receives the majority of its precipitation during the winter season. Berkelhammer and Stott (2008) and Bale (2010) both developed $\delta^{18}O$ tree ring records from Bristlecone Pines in the White Mountains of California, but with very different results. Berkelhammer and Stott (2008) recorded a dramatic decrease in $\delta^{18}O$ (~13‰) between 1850 and 1920, which they attributed to reduced occurrences of subtropical Pineapple Express storms. However, Bale (2010) recorded no such evidence of a dramatic shift in Pacific storm tracks. The ambiguity in the results may highlight the importance of proper site and tree selection to avoid the influence of biophysical effects, and the careful interpretation of results by comparing to other studies in nearby geographic regions.

Water resource management in a changing Pacific Northwest climate requires a strong grasp on how local climate responds to regional-to-global climate forcing patterns, and extending our knowledge beyond the instrumental record using proxy data is of key importance to providing a complete picture of future climate change within the context of past changes. The objective of this study is to develop an $\delta^{18}O$ tree ring record from

Douglas-fir (*Pseudotsuga menziesii*) for North Vancouver, BC and to (a) examine the differences between earlywood, latewood, and annual isotopic signatures, (b) place the record in context by comparing to other tree ring isotope records across the west coast of North America, and (c) discuss the potential sources of and influences on temporal variability in the tree ring oxygen isotope record, including source water, climate oscillatory behaviour and local meteorological conditions.

3.2. Materials and methods

3.2.1. Study area

The Capilano watershed spans 19,535 ha of the inland, mountainous area of North Vancouver (Figure 3.1). The watershed falls within the Coastal Western Hemlock (CWH) Biogeoclimatic zone of British Columbia, which is also the rainiest zone (Medinger and Pojar, 1991). The area receives a mean annual precipitation of 2043 mm, with mean annual temperature of approximately 9°C (1981-2000 climate normals; Environment Canada, 2013). Most of the annual precipitation falls over the winter months of October to March due to storm activity. From 1965-1985, Pineapple Express storms accounted for an average of 12% of the total annual precipitation, with some years contributing as much as 17% to annual rainfall (Chapter 2). The cool, moist climate creates ideal conditions for the western hemlock (*Tsuga heterophylla)* and Douglas-fir (*Pseudotsuga menziesii)* trees that dominate the landscape (BC Ministry of Environment, 1978). The Capilano watershed is a part of the dry maritime subzone (CWHdm), so major understorey species include salal (*Gaultheria shallon*) and red huckleberry (*Vaccinium parvifollum*). The submontane very wet maritime subzone (CWHvm1) occurs right above this zone, and has more Alaskan blueberry (*Vaccinium alaskaense*) present (Meidinger and Pojar, 1991).

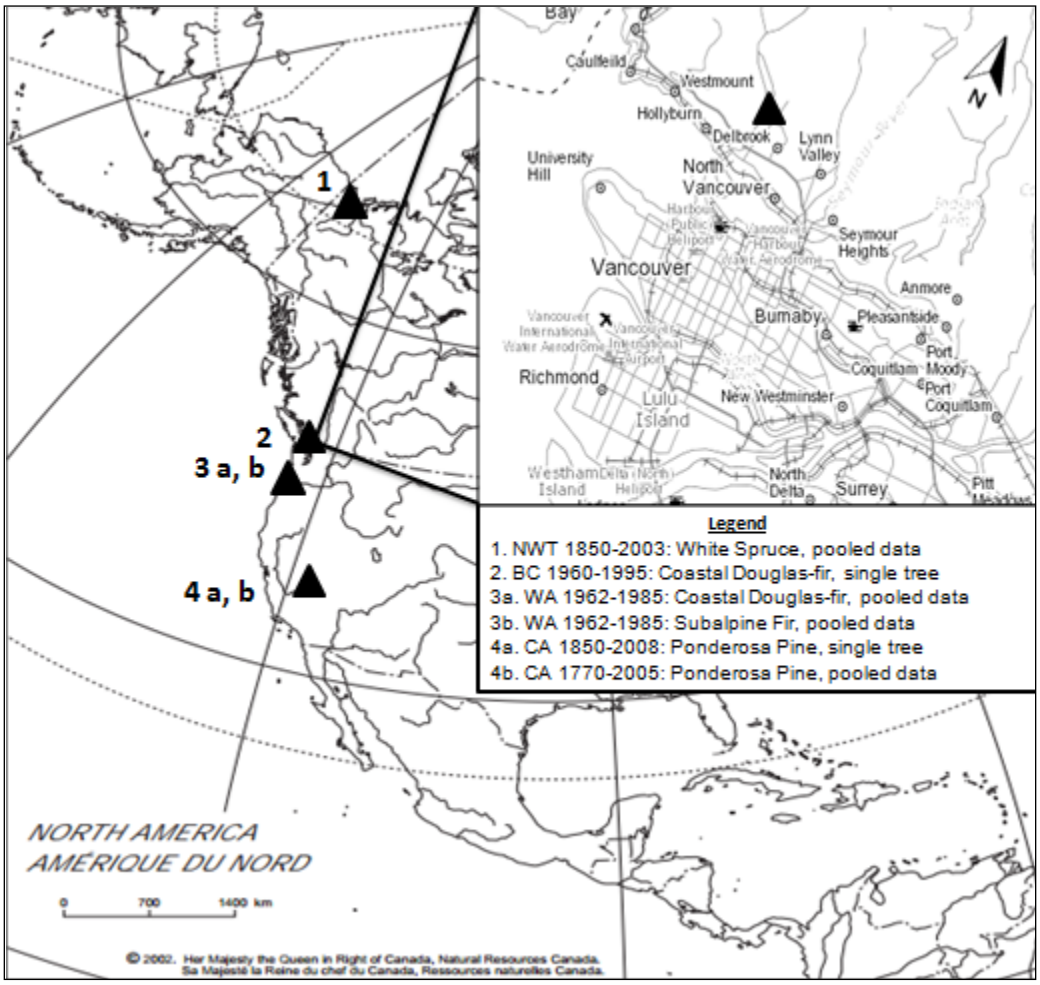

Figure 3.1. Map of western North America, showing the location of tree core sampling sites (▲) in the Northwest Territories (1), British Columbia (2), Washington (3a and 3b) and California (4a and 4b). The map to the right shows a detailed map of Metro Vancouver, BC and the sampling location of the Douglas-fir used in this study to reconstruct the oxygen isotope record from 1960-1995. Map images retrieved from the digital Atlas of Canada maps (Natural Resources Canada). The map is a reproduction of an official work published by Natural Resources Canada and has not been produced in affiliation with, or with the endorsement of, Natural Resources Canada.

In the summer and fall of 2010, four tree cores (DF1, DF2, DF3a and DF3b; Table 3.1) were sampled from three Douglas-fir trees in the Capilano River Regional Park (Site 2, Figure 3.1), using a five mm increment borer. Douglas-fir was selected as the species to sample because it is abundant in the region, and has large growth rings and distinct earlywood and latewood patterns (Martinez, 1996). The cores were sanded, dated using WinDendro software, and verified using the method established by Yamaguchi (1991) for living trees. Yamaguchi (1991) outlines a simple method for cross-

dating without using skeleton plots. The method involves listing narrow rings for each core, and comparing these listings to determine the local climatically controlled marker rings. Skeleton plots remain the method of choice for non-living trees in which year of the outer ring is not known and for regions that are prone to false or missing rings due to drought or monsoon conditions (Yamaguchi, 1991). The DF3a core was chosen from a tree that appeared representative of average stand conditions. The core was used to generate a modern record of $\delta^{18}O$ of tree ring cellulose that overlaps with a time period that is well documented by historical records, for which regional variability in precipitation source and overall climate is better understood.

Table 3.1. Site information and tree characteristics for the four tree cores sampled from three Douglas-firs in the Capilano River Regional Park.

Sample Name	DF1	DF2	DF3a	DF3b
Sampling Date	07/13/2010	07/13/2010	09/23/2010	09/23/2010
GPS Location	49°21'24" N 123°06'45" W	49°21'17" N 123°06'40" W	49°21'18" N 123°06'43" W	49°21'18" N 123°06'43" W
Elevation	90 m	60 m	67 m	67 m
DBH	3.46 m	2.40 m	2.17 m	2.17 m
Tree height	51.5 m	49.0 m	41.0 m	41.0 m
Tree Age	>84 years	123 years	141 years	141 years
Slope	7° N/NE	3° E/SE	4° E/SE	4° E/SE

3.2.2. Extraction of α-cellulose for oxygen isotope measurements

The years 1960-1995 were selected for analysis to allow for overlap with available meteorological data at the North Vancouver Capilano climate station (1955-1990). Each annual ring from the DF3a core was subdivided into earlywood and latewood sections, to better capture the seasonality of storm precipitation in the Metro Vancouver area. Earlywood is the "spring wood" and is the portion of the ring most likely to capture winter storm precipitation, whereas latewood is the "summer wood" that grows later in the season and into the early fall. Earlywood and latewood samples were finely ground, and α-cellulose was isolated from the wood using a modified version (Miller et al., 2006) of the extraction process established by Loader et al. (1997). The ground

wood samples were placed into Soxhlet extraction tubes with acetic acid and sodium chlorite. The tubes were then placed in a heated ultrasonic bath, which breaks down the wood into holocellulose by removing lipids, resins, tannins and lignins. The holocellulose was then placed in another ultrasonic bath with a sodium hydroxide solution to leach carbohydrates, such as mannan and xylan from the holocellulose, resulting in α-cellulose.

The α-cellulose samples were sent to the Saskatchewan Isotope Laboratory at the University of Saskatchewan for oxygen isotope analysis. Samples were analyzed using a Thermo Finnigan Temperature Conversion Elemental Analyzer coupled with a Conflo III and a Delta Plus XL mass spectrometer. Samples were pyrolyzed at 1450°C, releasing a carbon monoxide gas that is passed into the mass spectrometer that measures its oxygen isotope content. Isotopic measurements are reported as $\delta^{18}O$ (‰), relative to the VSMOW standard. The accuracy of this method is 0.11‰. In some cases, there was insufficient material from either the earlywood or latewood to complete the analysis. In this case, annual samples were measured from the supplementary DF3b tree core, which is from the same tree as DF3a. The missing earlywood or latewood values were then back-calculated, based on their weighted contributions to the annual ring. Similarly, the earlywood and latewood values were used to calculate the weighted, annual isotope values from 1960-1995.

3.2.3. Analysis of seasonal and annual tree ring isotope records

To examine the potential influence of Pineapple Express (PE) storm precipitation on tree ring isotope values, a linear regression was used to compare the earlywood, latewood, and annual isotope records to different PE variables (average vapour transport, average path length, average west coast crossing, and percent of PE precipitation; Table 3.2). The variables selected can be considered as different measures of PE intensity, because vapour transport represents the rate of subtropical moisture flux, and average path length measures the subtropical nature of the moisture source. The west coast crossing records PE storms making landfall in and around the Vancouver, BC area, while the percent of PE precipitation measures the contribution of PE storms to the annual water budget. In Chapter 2, the isotopic signatures of PE storms in Metro Vancouver were found to be on average of 5-6‰ more enriched than

winter storms originating in the North Pacific. Since PE storms can contribute >17% of the annual precipitation in Capilano (Chapter 2), it was reasoned that the tree ring isotope records for these years should be isotopically more enriched as well.

Table 3.2. Description of source water (PE) and climate oscillation variables used for linear regression analysis.

Variable (WY[1])	Description	Source
Source Water (PE) Variables		
Average Vapour Transport	Daily average vertically integrated water-vapor transport rate, along the back trajectory with largest average transports. Values are calculated from NCEP Reanalysis data and reported in kg/m/s (Dettinger, 2004).	Dettinger (2008)
Average Path Length	The number of 2.5º grid cells traversed along the back trajectory to reach either the southern terminus or 20°N (whichever was reached first; Dettinger, 2004).	Dettinger (2008)
Average West Coast Crossing	The latitude at which the trajectory with largest transport rate crossed the west coast (Dettinger, 2004).	Dettinger (2008)
Percent PE precipitation	The percentage of the total annual precipitation at the Environment Canada North Vancouver Capilano station (Climate ID 1005655) that resulted from the occurrence of PE storm (occurred on the day of, before or after a Dettinger, 2008 PE day). Values were calculated for 1965-1985, the time period when data were available.	Chapter 2
Climate Oscillation Variables		
MJO	The Madden Julian Oscillation (MJO) is an intra-seasonal oscillation (~20-90 days) in the equatorial Pacific, resulting in regions of enhanced and suppressed tropical precipitation (Madden and Julian, 1994; Mo, 2011). Data for the MJO Index were only available from 1979 onwards and are based on principal component analysis of the band pass filtered 30-day 850 hPa zonal wind of the equatorial (5°N – 5°S) (Maloney and Kiehl, 2002; NOAA, 2003).	NOAA (2003)
PDO	The Pacific Decadal Oscillation (PDO) a multi-decadal oscillation in sea surface temperatures (SSTs), with the positive phase representing a deepening of the Aleutian Low and an intensified SST gradient between the cool western and warm eastern Pacific (Mantua et al. 1997). The PDO Index (Zhang et al., 1997, Mantua et al., 1997) is defined as the primary component of SST variability in the Pacific Ocean, poleward of 20°N (Joint Institute for the Study of Atmosphere and Ocean (JISAO) 2012).	JISAO (2012)
ENSO	El Niño Southern Oscillation (ENSO) is a 3-7 year oscillation, with high sea surface temperatures (SST) and atmospheric pressure anomalies occurring during the warm El Niño phase in the eastern tropical Pacific (Trenberth, 1997). The ENSO 3.4 Index refers SST anomalies in the El Niño 3.4 Region, which is bound by 120°W-170°W and 5°S- 5°N (Trenberth,1997; University Corporation for Atmosphere Research (UCAR), 2012).	UCAR (2012)

Variable (WY[1])	Description	Source
AO	The Arctic Oscillation (AO) is the dominant pattern of non-seasonal sea-level pressure (SLP) variations north of 20°N, and is characterized by SLP anomalies of one sign in the Arctic and anomalies of opposite sign between 37°N and 45°N (Mitchell,2004). The indices are generated by projecting anomaly fields onto the structure of the AO, defined as the primary component of SLP poleward of 20°N based on all months (January 1958-April 1997; Thompson, no date).	Thompson, no date.
NPGO	The North Pacific Gyre Oscillation (NPGO) is a decadal-scale climate oscillation that is defined as the second dominant mode of sea surface height anomalies in the Northeast Pacific, after the PDO. Fluctuations in the NPGO are strongly influenced by wind-driven upwelling, and are significantly correlated with physical and biological parameters (salinity, nutrients and chlorophyll-a; Di Lorenzo et al., 2008).	Di Lorenzo et al., 2013
PNA	Pacific/North American (PNA) teleconnection pattern is one of the most recognized modes of low-frequency variability in the Northern Hemisphere extratropics. The PNA is characterized by opposing geopotential height anomalies over western and eastern North America. The PNA has been found to be strongly influenced by ENSO and is associated with strong fluctuations in the strength and location of the East Asian jet stream (NOAA, 2012).	NOAA, 2013
Meteorological Variables		
Average Temperature	Mean monthly temperatures from Environment Canada's West Vancouver Capilano GCC station (Climate ID 1108825). Data were available from 1976-1998.	Environment Canada, 2013
Total Precipitation	Cumulative precipitation totals recorded at Environment Canada's North Vancouver Capilano station (Climate ID 1005655). Data were available from 1964-1986.	Environment Canada, 2013

[1] WY = Water year; variables were averaged over each water year (October-September).

To examine the potential influence of regional climate oscillations on tree ring isotope behaviour, a linear regression analysis (Pearson r) was also used to compare the seasonal and annual tree ring isotope records to different climate oscillation indices influencing the Pacific Northwest: Madden Julian Oscillation (MJO), Pacific Decadal Oscillation (PDO), El Niño Southern Oscillation (ENSO), Arctic Oscillation (AO), North Pacific Gyre Oscillation (NPGO) and the Pacific/North American teleconnection (PNA; Table 3.2). Both the source water (PE) and climate oscillation variables were averaged over each water year (October-September) to capture the seasonality of the precipitation that would be influencing tree ring growth. Average temperature and total precipitation

for each water year were also included in the analysis, to capture meteorological variables that influence the local climate.

To place the observed record within the context of other regional climate archives, the annual tree ring isotope record was compared to records from across western North America, including sites from the Northwest Territories (Porter, 2009), Washington State (Shu et al., 2005) and California (Bale et al., 2010; Figure 3.1). Porter (2009) used six cores from three White spruce (*Picea glauca*) trees on the Mackenzie Delta to develop three annual oxygen isotope records for 1850-2003. The mean of the three records was calculated to establish an average annual record for the region, referred to in this study as NWT. Shu et al. (2005) sampled Douglas-fir (DF; *Pseudotsuga menziesii*) and Subalpine fir (SAF; *Abies lasiocarpa*) trees from five different sites in the Olympic Mountains of Washington. For this study, an average annual record was created for each species (WA_DF and WA_SAF) by calculating the mean values from 1962-1985, using only complete records with no missing data for the calculation. Bale et al. (2010) sampled bristlecone pine (*Pinus longaeva*) from the White Mountains of California during field work in July 2004, July 2005 and July 2008, and developed a single-tree record (Methuselah, 1850-2007) and a pooled record (Blanco, 1770-2005). The pooled record was established by combining equal amounts of α-cellulose from six living bristlecone pine trees into a single homogenized sample. In this study, the Bale (2010) records will be referred to as CA_M and CA_B.

The various records were then analyzed for any long-term trends, comparing each of these geographic records from across western North America to the observed annual record from British Columbia using a linear regression (Pearson r). As well, a hierarchical cluster analysis was conducted in the R statistical package using a Manhattan distance measure to further investigate the relationships between the isotope records (Maechler, 2013).

3.3. Results

3.3.1. Seasonal and annual tree ring isotope record for Vancouver, BC (1960-1995)

Between 1960 and 1995, the oxygen isotope values ranged from 18.3 to 26.3‰ for the earlywood and from 16.8 to 24.0‰ for the latewood (Figure 3.2), with latewood values being an average of 1.3‰ more enriched than the earlywood values (24.2‰ compared to 22.9‰; Appendix). The annual values were estimated as the weighted mean of the two seasonal (earlywood and latewood) measurements, with the exception of eight years in which annual measurements were made directly (Appendix). In general, the annual values are slightly more closely related to the latewood isotope values, because the latewood contributed a mean of 56% to the mass of the total annual ring.

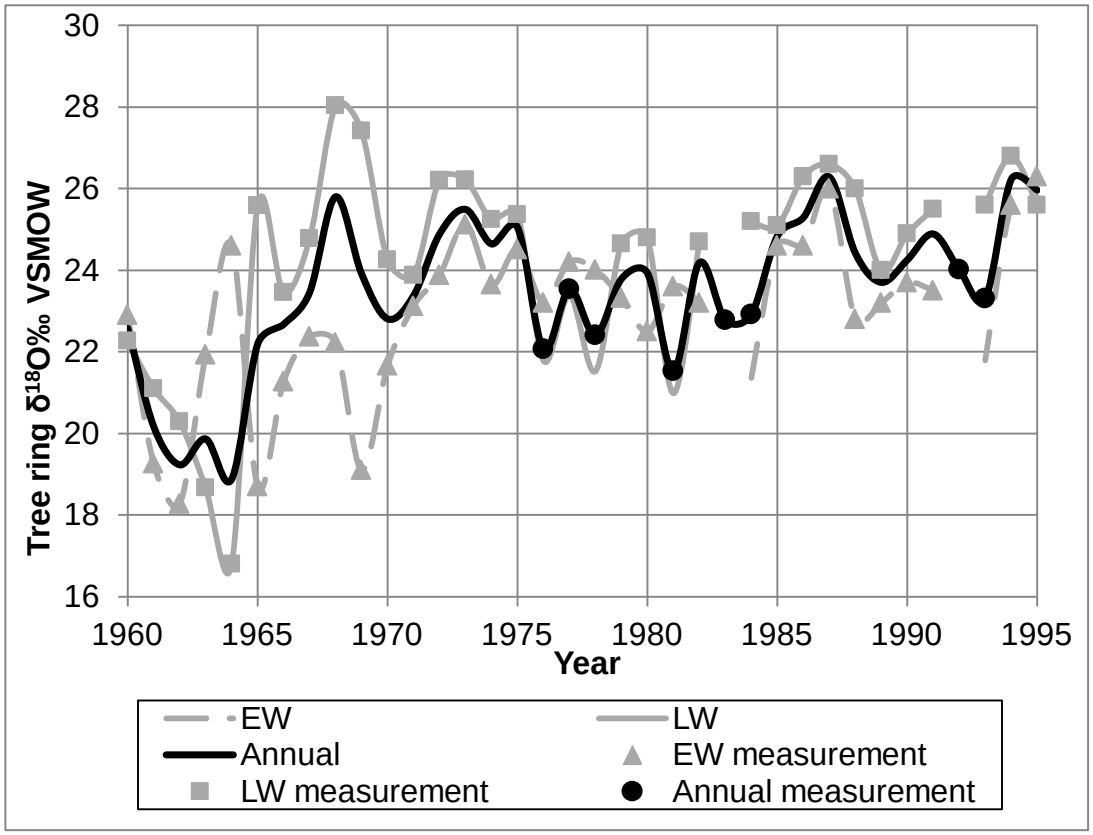

Figure 3.2. Earlywood (EW), latewood (LW) and annual tree ring isotope values for Vancouver, BC (1960-1995). Data points indicate laboratory measurements, and no data point indicates calculated values.

The records can be divided into two different phases, prior to 1970 and post-1970. Post-1970, all the records are fairly stable and fluctuate within a 5‰ range. Prior to 1970, however, the records are highly variable from year to year, and the range for the latewood values is greater than 10‰. As well, the years 1960-1965 show the most depleted values of the entire length of the record, for both the seasonal and annual records. For the majority of the record, latewood values are more positive than the earlywood values. A major exception to this pattern occurs in years 1963 and 1964, when $\delta^{18}O$ measurements for the latewood are substantially more depleted than the earlywood.

3.3.2. Relationships with source water, climate oscillations and meteorological variables

Results from linear regression analysis indicate no significant correlations between Pineapple Express (PE) characteristics and seasonal and annual tree ring $\delta^{18}O$ values (Table 3.3). Years with powerful PE storms (high average vapour transport rate), distinct subtropical moisture sources (high average path length), PE storms in close proximity to the Vancouver area (high west coast crossing) and strong PE contribution to the annual water budget (high percent of PE precipitation) do not result in significant enrichment of tree ring $\delta^{18}O$ isotope values. Very few, but some significant, relationships are found between the tree ring isotope records and climate oscillation indices, including the NPGO, the MJO, and the AO. The NPGO is significantly negatively correlated to both the annual ($r= -0.34$, $p< 0.05$) and latewood ($r= -0.42$, $p <0.05$; Table 3.3) isotope records. The latewood record is also negatively correlated with the MJO ($r= -0.35$, $p< 0.05$), and the earlywood is correlated with the AO ($r=0.37$, $p<0.05$; Table 3.3). With regards to meteorological variables, a significant relationship between the average temperature and earlywood values was also noted.

Table 3.3. Pearson r coefficients and p values for the linear relationships between earlywood (EW), latewood (LW) and annual δ18O with source water (PE) variables and climate oscillation indices, averaged over the water year (WY), October-September (1960-1995). Significant relationships are shown in bold and with an asterisk.

Variable (WY)	**Annual $\delta^{18}O$**	**EW $\delta^{18}O$**	**LW $\delta^{18}O$**
Source Water (PE) Variables			
Average Vapour Transport	r= -0.24 p= 0.17	r= < -0.01 p= 0.98	r= -0.27 p= 0.12
Average Path Length	r= 0.14 p= 0.42	r= 0.27 p= 0.13	r= 0.06 p= 0.76
Average West Coast Crossing	r= -0.09 p= 0.60	r= 0.19 p= 0.29	r= -0.21 p= 0.24
Percent PE Precipitation	r= 0.04 p= 0.88	r= 0.18 p= 0.44	r= 0.02 p= 0.94
Climate Oscillation Variables			
MJO	r= -0.20 p= 0.46	r= 0.09 p= 0.63	**r= -0.35* p= 0.04***
PDO	r= 0.30 p= 0.07	r= 0.31 p=0.07	r= 0.28 p= 0.11
ENSO	r= 0.10 p= 0.55	r= 0.06 p= 0.75	r= 0.12 p= 0.49
AO	r= 0.25 p= 0.15	**r= 0.37* p= 0.03***	r= 0.12 p= 0.46
NPGO	**r= -0.34* p= 0.04***	r= 0.01 p=0.97	**r= -0.42* p= 0.01***
PNA	r= -0.11 p= 0.52	r= 0.02 p= 0.90	r= -0.12 p= 0.51
Meteorological Variables			
Average Temperature	r=0.39 p=0.10	**r=0.69* p=0.001***	r=0.06 p=0.80
Total Precipitation	r=-0.13 p=0.56	r=0.10 p=0.65	r=0.09 p=0.70

3.3.3. Geographic comparison of western North America tree ring records

When all tree ring $\delta^{18}O$ records from the Northwest Territories (NWT), British Columbia (BC), Washington (WA_SAF, WA_DF) and California (CA_B, CA_M) are plotted together (Figure 3.3a), the average $\delta^{18}O$ values demonstrate a pronounced dependence on latitude. The northern NWT record is the most depleted in $\delta^{18}O$ followed by BC, Washington and finally the California records, which are the most enriched in $\delta^{18}O$. Examining a subset of the data from 1962-1985, when all of the geographic records overlap, allowed investigation of inter-annual trends and relationships. Figure 3.3b demonstrates that the Washington records are very similar in terms of their isotopic signatures and temporal trends, despite the samples being taken from different species. In contrast, the California records seem to be less closely related and have higher interannual variability. The BC annual record contains values that are more similar to those found in the NWT in some years and the California records in other years. The BC record does not appear to closely mirror one record over the other, although it does have higher interannual variability like the California records. The depleted values in the BC record from 1960-1965 are not experienced by any other record. In fact, these values are the lowest of all the records, surpassing even the NWT record in 1962 and 1964.

Some significant and sustained long-terms trends are observed in some of the records. For example, both of the California records appear to be becoming isotopically depleted, with CA_B at a rate of -0.008‰/year and CA_M at -0.019‰/year. Both of these trends are significant ($p < 0.05$). For the entirety of the CA_B record, this rate amounts to an average change of almost -2‰ from 1770-2005. On the other hand, the NWT record is becoming isotopically more enriched (0.010‰/year from 1850-2003, $p < 0.05$). The BC and WA_DF records also demonstrate a slight trend towards becoming isotopically enriched as well, at 0.106 and 0.034‰/year, respectively. Both of these trends are significant at the 95% confidence level.

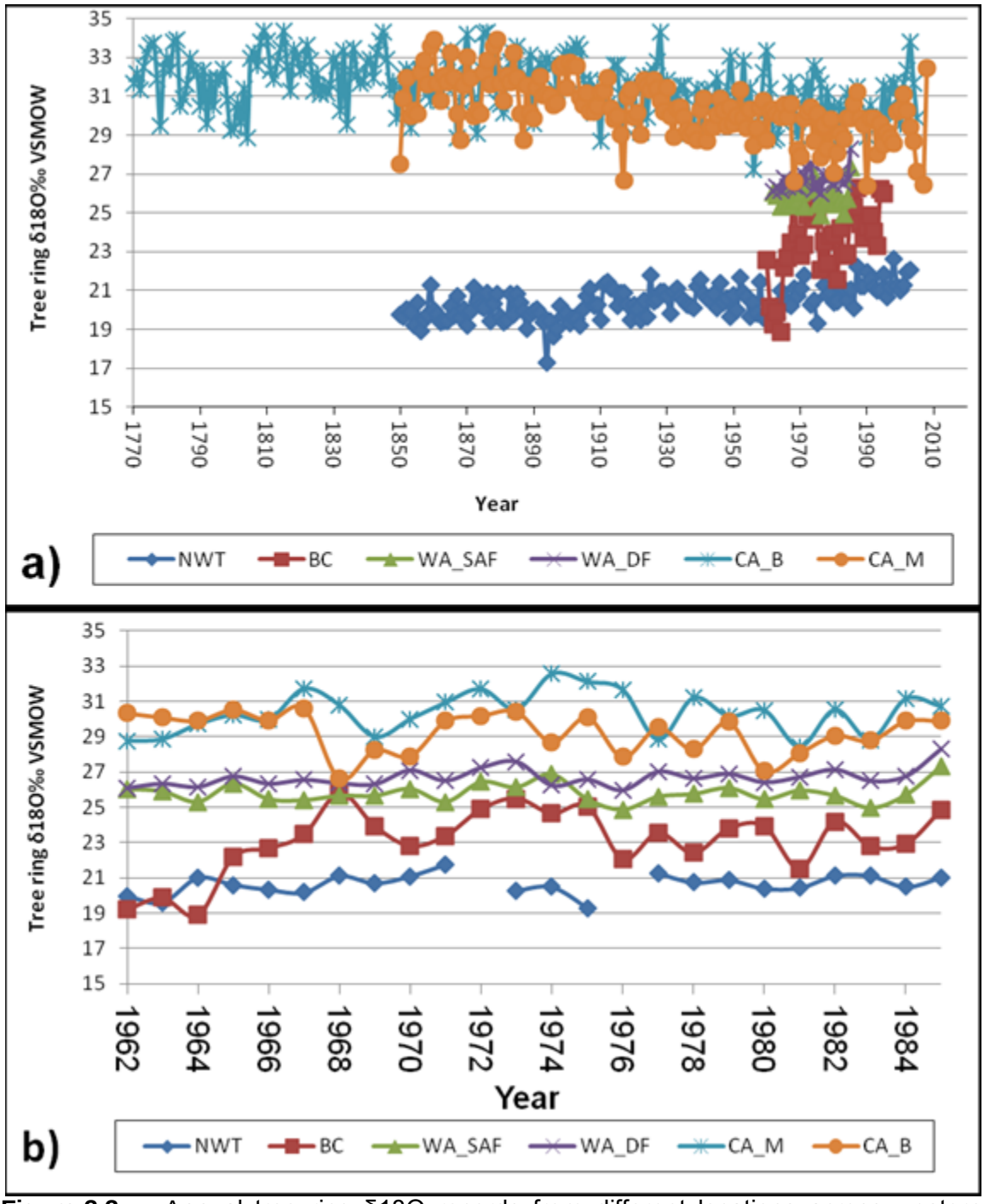

Figure 3.3. Annual tree ring δ18O records from different locations across western North America: Northwest Territories (NWT; Porter, 2009), British Columbia (BC), Washington (WA_SAF, WA_DF; Shu et al., 2005), and California (CA_B, CA_M; Bale et al., 2010). The isotope records are presented (a) in their entirety, from 1770-2008 and (b) over the time period when they all overlap, from 1962-1984.

Results from the linear regression analysis (Table 3.4) indicate that the annual tree ring $\delta^{18}O$ signatures in Vancouver are significantly correlated to the NWT signature ($r= 0.40$, $p= 0.02$), and have a significant negative relationship to both California records. The earlywood values are also correlated with NWT values, while latewood values have no significant relationships to the other tree ring records. The Washington and BC records are not significantly correlated, despite their geographic proximity and species type (Douglas-fir). The results of the cluster analysis echo the regression analysis, and suggest that the annual BC record is, in fact, more closely related to the NWT than to WA or CA (Figure 3.4). The hierarchical cluster groups the Canadian and American records together, and then subdivides the American records into WA and CA groups.

Table 3.4. Pearson r coefficients and p values for the linear relationships between tree ring $\delta^{18}O$ records from Vancouver, BC (annual, earlywood latewood) and other tree ring $\delta^{18}O$ records from across western North America: Northwest Territories (NWT; Porter, 2009), British Columbia (BC), Washington (WA; Shu et al., 2005), and California (CA; Bale et al., 2010). Significant relationships are shown in bold and with an asterisk.

Tree ring record	Annual BC	Earlywood BC	Latewood BC
NWT	**0.40*** **p= 0.02**	**0.37*** **p= 0.03**	0.32 p= 0.06
WA_SAF	-0.06 p= 0.78	0.048 p= 0.83	0.26 p= 0.23
WA_DF	0.24 p= 0.26	0.40 p= 0.05	0.37 p= 0.08
CA_B	**-0.26*** **p= <0.01**	0.27 p= 0.13	0.23 P= 0.20
CA_M	**-0.33*** **p< 0.01**	0.02 p= 0.90	-0.08 p= 0.66

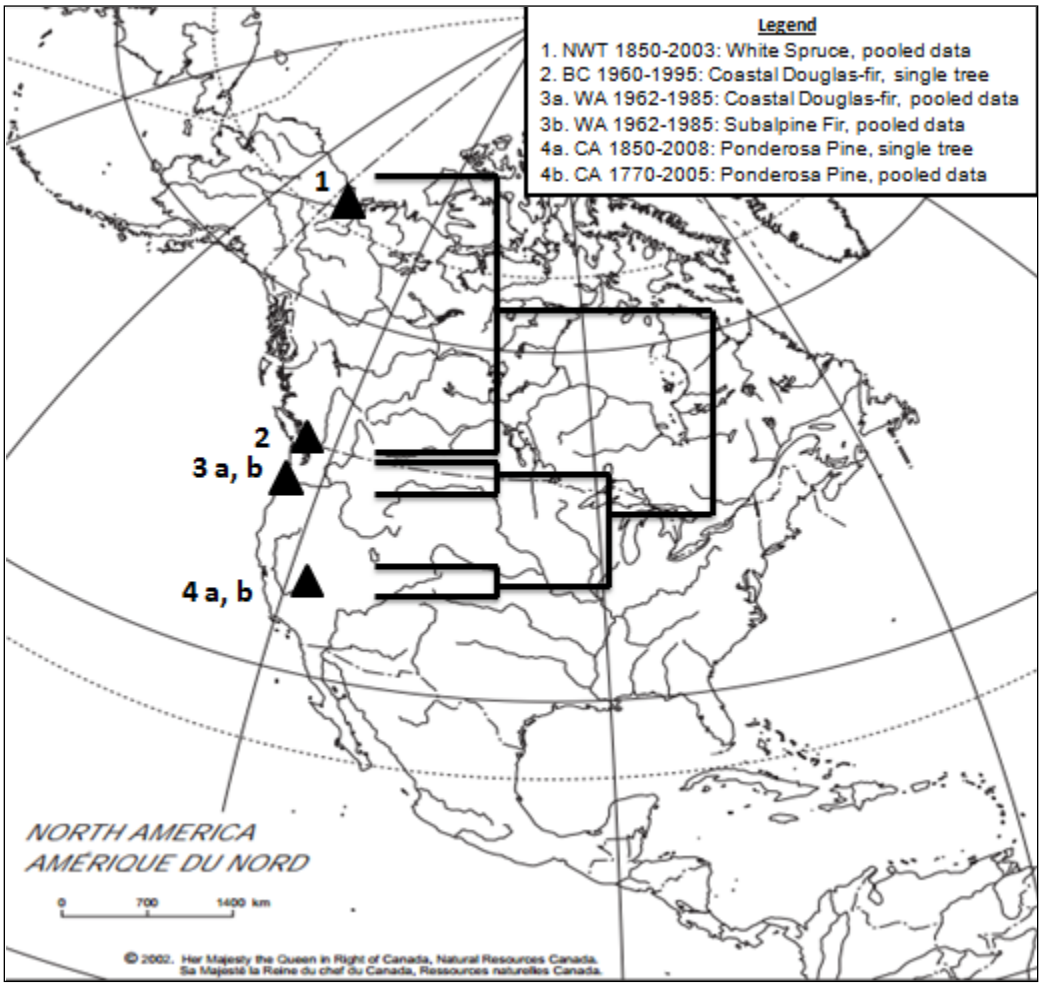

Figure 3.4. Grouping of tree ring oxygen isotope records from across western North America using hierarchical cluster analysis. Map image retrieved from the digital Atlas of Canada maps (Natural Resources Canada). The map is a reproduction of an official work published by Natural Resources Canada and has not been produced in affiliation with, or with the endorsement of, Natural Resources Canada.

3.4. Discussion

3.4.1. Seasonal variability in isotope precipitation

The latewood oxygen isotope ratios from 1960-1995 are an average of 1.3‰ more enriched than the earlywood. Isotopic sampling of bulk monthly precipitation data for a nearby GNIP (Global Network of Isotopes in Precipitation) station on Saturna Island, BC (IAEA/WMO, 2013) indicates that precipitation in other parts of coastal British Columbia experience a similar degree of isotopic variability as is seen in the tree ring

records for North Vancouver. Spring precipitation (April, May and June) averages -9.6‰ and summer precipitation (June, July and August) averages -8.0‰, equating to a difference of 1.6‰. The winter and fall isotope ratios for precipitation are typically more depleted (-12.1‰ and -8.3‰, respectively), so one might expect a larger offset between earlywood and latewood if the earlywood is up taking stored winter precipitation as well.

If we assume that the biophysical effects on isotopic fractionation are the same for the same tree in the same environment (Anderson et al., 2002), then the comparable size between the spring/summer and earlywood/latewood offsets may indicate that the isotopic signature of earlywood in Douglas-firs in North Vancouver are recording Spring rather than stored winter precipitation. The seasonal variability in tree ring and precipitation isotope ratios is essentially a function of temperature, as summer (latewood) reflects a warmer climate than spring (earlywood). Other studies have documented temperature controls over isotope ratios manifested as differences in source water, such as subtropical PE storms being isotopically more enriched than those originating from the subpolar North Pacific Ocean (Chapter 2; Berkelhammer and Stott, 2008).

3.4.2. Temporal trends in North Vancouver's isotope record

The annual records from the tree core collected in this study exhibit an increasing trend of 0.106‰/year from 1960-1995. However, the record as a whole can be clearly divided into two distinct phases: 1960-1970 ("pre-1970") and 1971-1995 ("post-1970"), and the difference in means between these two time periods is statistically significant ($p<0.05$). Before 1970, the higher interannual variability and anomalously depleted isotope values in 1962, 1963 and 1964 drive the trend. The latter stage of the record displays consistent earlywood and latewood behaviour, and no significant trends from 1970-1995. The phase shift could be a record of a change in climate, or it could be the result of a change in environmental conditions of the tree's environment, such as nutrient availability, light, or disturbance in the area (Singer et al., 2013; Jansen et al., 2013; McCarroll and Loader, 2004). Lepofsky et al. (2003) identified an abrupt initiation in the 1970s of tree encroachment into the Chittenden Meadow near Hope, BC. The encroachment was coincident with changes in spring climate (higher temperatures and lower snowpack) recorded in Washington State, and lack of fire in the area, which likely

helped conifer seedlings survive the hot, dry summer. The tree ring isotopes could be recording the same change in regional climate that was identified by Lepofsky et al. (2003).

The tree ring annual growth in mm from 1960-1995 is significantly correlated ($r= -0.46$, $p < 0.05$) to the isotope record. However, years with the anomalously depleted isotope values (1962, 1963 and 1964) experiences growth rates of 1.90, 2.35 and 4.03 mm/year. These tree ring growth rates are within the range of the rest of the isotope record (0.90- 4.04 mm/year) and similar to the mean (1.97 mm/year). Therefore, the growth rates suggest that a process other than a change in environmental conditions of the tree is responsible for the isotopic phase shift pre- and post-1970. Another possible explanation for the phase shift is the potential cross-contamination of samples due to human error while dating and separating the seasonal samples, or conducting the α-cellulose extraction in the laboratory. More investigation into these matters is needed to verify the results, and may require collecting and analyzing isotopes in tree rings from multiple additional Douglas-firs in Capilano River Regional Park or elsewhere locally. Re-sampling can provide clarity regarding isotope results; for example, Berkelhammer and Stott (2008) are further investigating their Bristlecone Pine $\delta^{18}O$ record from California after Bale (2010) identified contrary results. Future sampling of Douglas-firs in Vancouver, BC could create a pooled record, which could help to resolve the variability between individual trees and present a regional average for the site (Bale, 2010).

3.4.3. Source water isotopic controls over tree ring $\delta^{18}O$ values

No significant correlations were found between the annual and seasonal tree ring $\delta^{18}O$ records and any of the source water variables, despite the significant contribution of Pineapple Express storms to the water budget (Chapter 2). Based on a simple conceptual infiltration model, it is estimated that it would take up to 289 days (approximately 9 and a half months) for winter storm precipitation to reach a depth of 2.5 m, which is the maximum rooting depth for Douglas-firs in humo-ferric podzol (Crow, 2005; Pojar et al., 1991). The infiltration model is based on Darcy's law, in which the infiltration rate of soil (Q) becomes equal to the hydraulic conductivity (K) of the geologic substrate during saturated conditions (Dingman, 2002). Groundwater levels from a groundwater observation well in Belcarra, BC (BC Observation well #349, BC Ministry of

Environment, 2013) indicate saturated groundwater conditions over the winter season from October to May, so a K-limited infiltration model is appropriate. The soil thickness is estimated to be approximately 1 m, with granitic bedrock underlying the soil. Given that bedrock has a significantly lower K of ~10^{-7}m/s (Brox et al., 2004; Haught, 2010) compared to soil (Clapp and Hornberger, 1978; Mecke and Ilvesniemi, 1999; Oosterbaan & Nijland, 1994), the bedrock permeability becomes the limiting factor for infiltration.

Based on this simple conceptual infiltration model, winter storm precipitation would infiltrate the soil / bedrock at a steady rate during saturated conditions of the winter season, and it would take 289 days for water to travel to 2.5 m depth. The substrate would contain a mixed isotopic record of winter storm precipitation, and trees would have access to stored soil water from a maximum of 289 days prior. However, much of the precipitation from large storm events is lost to run-off, so the substrate water isotope values would not be a weighted representation by storm precipitation amount, but rather could be biased towards precipitation events that are of low intensity and long duration. As well, since the substrate is still saturated in Spring when the growing season for Douglas-firs begins, it is possible that the fine network of roots is drawing water from the shallow soil zone instead of relying on the larger roots to draw from the deeper reserves. The shallow fine roots are the primary source of nutrients (since most decomposition and nutrient mineralization occurs in the organic layers or near the surface of the mineral soil), but they also take up water when the soil around them is wet (Brooks et al., 2010). Later in the season when the surface soil dries, the roots may reach deeper reserves of winter recharge.

In summary, the use of oxygen isotope values in tree rings as a proxy for tropical cyclone activity in the southeastern U.S. (Miller et al., 2006) is not an effective method for recording PE storm activity along the west coast. Unlike cyclones, PE storms occur over the winter season, which corresponds to the dormant season for tree growth. The lag between the timing of the storm event and the growing season for trees leads to a loss of PE isotopic signature to groundwater, runoff and isotopic mixing. The result is no significant relationship between PE variables and the $\delta^{18}O$ α-cellulose measurements.

Multiple studies have also identified summer fog as an important source of moisture in coastal ecosystems (Roden et al., 2009; Dawson, 1998; Johnstone et al., 2013), yet it was not included in this analysis. In particular, the coast redwood (*Sequoia sempervirens*) is known to have a seasonal reliance on fog as a hydrologic input during the dry California summers. Mature redwood forests have been estimated to obtain 22-46% of their annual hydrologic input from fog through the fog drip from the tree itself, which is known as an interception input (Roden et al., 2009; Dawson, 1998). The summer fog (-1‰) is isotopically enriched in ^{18}O relative to winter precipitation (-8‰) in California and coincides with seasonally enriched latewood values in tree ring records (Johnstone et al., 2013; Dawson, 1998). Within an annual tree ring, ^{18}O values tend to be depleted (precipitation) near the tree ring boundaries and most enriched (fog) around the center because of seasonal differences in hydrologic input (Roden et al., 2009). For this reason, middlewood has been used for dendroclimatic studies on fog because it corresponds to the time of the growing season in which trees are most dependent on fog as a hydrologic input (Johnstone et al., 2013) Therefore, this would also infer that dendroclimatic studies on winter precipitation should use the portions of the tree ring closest to the ring boundary. Future research could investigate the implications of analyzing different portions of the annual tree ring to better target specific times of the year and particular hydrologic inputs. Also, the tree ring research presented in this study would benefit greatly from quantitative research on fog as a hydrologic input to trees in coastal British Columbia.

3.4.4. Role of climate oscillations

No significant relationships were observed between the PDO, ENSO or PNA and annual and seasonal tree ring $\delta^{18}O$ records from Vancouver, BC. The PNA and PDO are low frequency climate oscillations, so it is possible that the short length of the records (35 years) does not capture enough of the variability in the low frequency records to have a significant relationship. As well, the PNA is strongly influenced by ENSO (NOAA, 2012), so it is fitting that no significant correlations with ENSO will also result in no significant correlations with the PNA.

Significant relationships between the MJO and latewood (r= -0.35), the AO and earlywood (r= 0.37) and the NPGO and latewood (r= -0.42) and annual tree ring $\delta^{18}O$

values (r= -0.34) were observed. The MJO is strongly tied to the summer Indian monsoon season in the Northern Hemisphere (Pai et al., 2011), which is consistent with the negative correlation observed. During the negative MJO phase, isotopically enriched precipitation is recorded in the latewood record because the convective region is displaced to the western Indian Ocean. As the MJO propagates eastward (Mo, 2011), a positive MJO phase is observed and the tree ring oxygen measurements become isotopically depleted.

The association found between the NPGO and the latewood and annual records could result from the documented influence of the NPGO on gyre circulations, wind patterns, and associated storm behaviour in the North Pacific. For example, recent studies have found a link between the NPGO and seasonal changes in wind patterns and upwelling along the west coast (Bylhouwer at al., 2013). As well, the positive phase of the NPGO is known to be associated with enhanced wind and upwelling in the California Current System, south of 38°N (Di Lorenzo, 2008). Our results indicate that the positive NPGO phase is strongly correlated to more depleted oxygen isotope ratios in the latewood and annual records, and depleted isotope values are characteristic of storm activity (Miller et al., 2006; Jouzel et al., 2003). Storm events can lead to strong currents and coastal upwelling (Carton, 1984; Mathis et al., 2012), so therefore our results are consistent with these previous studies.

Both the NPGO and MJO are subtropical/temperature in nature, and correlations with the latewood suggest a distinct lower-latitude control over the record in the summer and early fall. However, we have also identified a strong link between earlywood and AO which suggests a northern influence over the record earlier in the season. British Columbia appears to be in a located in transitional mid-latitude zone, with climate and weather patterns arriving from the north and the south. The relative strength of each of these regional influences will vary depending on the time of year.

It is difficult to attribute the variability in tree ring isotopes to an individual climate oscillation because the reality is that the different oscillations occur simultaneously, yet on very different time scales. For example, when ENSO and PDO are both in positive phases, they have a positive feedback effect and reinforce one another (Wang et al., 2006). However, the period of ENSO variability is short (3-7 years) while the PDO is long

(20-30 years). When the oscillations are out of phase with each other, they create a negative feedback effect (Dettinger, 2001). Teasing out individual relationships between a given climate index and the tree ring isotope ratios is challenging because the annual $\delta^{18}O$ values are actually recording the net effect of the oscillations influencing the regional climate of coastal British Columbia. When the PDO and ENSO Indices are normalized and averaged into a single index, the strength of the correlation increases significantly ($r= 0.24$, $p= 0.16$) compared to considering only the ENSO Index ($r= 0.10$, $p= 0.55$). The correlation could perhaps be strengthened in the future by the addition of other climate oscillations that help to explain the variance in tree ring isotope values, and by considering different weightings of each oscillation. However, this study does provide an indication of which climate oscillations have the strongest influence on oxygen isotope ratios (MJO, NPGO and AO).

3.4.5. Spatial relationships and the Rayleigh distillation effect

When plotted together, the average $\delta^{18}O$ values from the annual tree ring records from western North America demonstrate a pronounced dependence on latitude. A distinct meridional temperature gradient exists along the west coast of North America, and this gradient has a strong influence on the ratio of isotopes in precipitation due to the Rayleigh distillation effect. When water condenses out of a cloud, the heavy isotope (^{18}O) is preferentially rained out over the light one (^{16}O; McCarroll and Loader, 2004). The process continues as a storm travels along its trajectory, which leads to the precipitation becoming increasingly depleted in ^{18}O because most of it has already been condensed out of the air mass (Jouzel et al., 2003). Therefore, precipitation amount, latitude, elevation, and distance from the coast all enhance the Rayleigh distillation effect. This effect is reflected in the tree ring isotope records, which became more depleted in ^{18}O with increasing latitude along the west coast of North America. The magnitude of the effect from the White Mountains of California (CA_B) to the Mackenzie Delta in the Northwest Territories (NWT) is approximately 10‰ over 30° of latitude (0.33‰/°) on average. These results are comparable to the magnitude of the effect documented in $\delta^{18}O$ in precipitation by GNIP. From 1961-1999, the mean weighted annual $\delta^{18}O$ values in western North America are approximately 11‰ more depleted at 60°N than 30°N (IAEA/WMO, 2013). This equates to rate of change of 0.37‰/° latitude.

3.4.6. Isotopic boundary

The Cluster analysis segregates the Canadian and American records, thereby suggesting that the BC record is more closely related to the NWT record than the Washington records which are geographically closer. The linear regression analysis echoes these results, identifying strong correlations between the NWT and BC records and evidence of the influence of northern climate over BC tree oxygen isotope ratios. Both of the Canadian records are negatively correlated to the California records, providing further support an isotopic boundary between Canada and the US. One possible explanation for the isotopic boundary is that it represents the southern reach of northern climate on west coast tree ring records.

The results are consistent with other studies that have also identified a disjunction between the northern and southern oceanographic conditions off the coast of British Columbia. For example, Peterman and Dorner (2012) identified a negative correlation between fish productivity in Alaska and southern BC over the two decades. The Fraser River sockeye salmon stocks across western North America have seen rapid and consistent decreases in productivity since the late 1990s. The trend is shared amongst most of the southern stocks across western North America, but are opposite of the trends occurring in western Alaska. Similarly, the Fraser Valley Fire Period (FVFP) is another example of a geographically localized climatic regime over the southern Straight of Georgia (Lepofsky et al., 2005). The FVFP is characterized by persistent summer drought and increased forest fires, and likely caused a rapid decline in salmon abundance. The FVFP coincides with a distinct period of cultural change known as the Marpole phase (2400-1200 BP), during which the necessary social and economic ties were built to diversify and manage resources in an uncertain climate. Man-made systems are intrinsically linked to climatic regimes and can therefore be impacted by changes in ocean-atmosphere conditions.

The boundary between the northern and southern ocean-atmosphere conditions is not stationary, so depending on climatic conditions such as PDO (Mantua et al., 1997), Vancouver's relative location to the boundary can shift from year to year. This could explain why the BC isotopic record is more strongly correlated with CA_B and CA_M in some year than NWT. Mantua et al. (1997) found evidence of reversals in the

polarity of the trend around 1925, 1947 and 1977, and the last two reversals also correspond to dramatic shifts in salmon production. Although an inverse relationship between the northern and southern oceanographic conditions off the coast of BC was found, the results of this study must be interpreted with caution.

First, the BC record is highly variable from 1960-1970, and this could potentially be the result of biophysical fractionation effects in the tree, or sample contamination. Like the NWT record, BC is showing a trend of becoming isotopically enriched from 1960-1995. Post-1970, however, there are no significant trends in any of the records over this time period. The possibility of biophysical effects or contamination causing variability at the beginning of the record cannot be ruled out, so it is possible that long-term trends are driving the observed correlations. As well, the NWT and CA records have an inverse relationship, but long-term trends suggest these records are actually converging. NWT is becoming isotopically more enriched, and California is becoming isotopically depleted. These trends could be the result of climate change decreasing the temperature gradient from the equator to the pole, thereby decreasing the magnitude of the Rayleigh effect. They could also influence the observed correlations between the tree ring isotope records and with climate indices. These questions can be resolved by resampling and possibly also extending the earlier portions of the tree ring isotope record.

3.5. Conclusions

This study demonstrates that oxygen isotopes in tree rings are effective tools for studying regional paleoclimate in coastal British Columbia. The Douglas-fir $\delta^{18}O$ annual record from North Vancouver identifies an isotopic phase shift in the early 1970s, which coincides with recorded temperature increases in nearby Washington State. The $\delta^{18}O$ record is not strongly correlated to source water variables (eg. Pineapple Express storms) or climate oscillatory behaviour, however it does demonstrate a strong regional climate signal driven by temperature and the Rayleigh distillation effect. Increases in latitude along the west coast of North America (from California to the North West Territories) result in increasingly more enriched isotope values. British Columbia sits on a boundary in the North Pacific Ocean between these inverted northern and southern

ocean-atmosphere conditions, and this boundary has been shown to shift over intra- and inter-annual time scales. Long-term trends indicate that the California and Northwest Territories $\delta^{18}O$ records are converging, which could be the result of climate change decreasing the temperature gradient between the equator and the poles.

3.6. References

Anderson, W. T., S. M. Bernasconi, J.A. MacKenzie, M. Saurer, and F. Schweingruber. 2002. Model evaluation for reconstructing the oxygen isotopic composition in precipitation from tree ring cellulose over the last century. *Chemical Geology* 182:121-137.

Bale, R. J. , I. Robertson, S. W. Leavitt, N. J. Loader, T. P. Harlan, M. Gagen, G. H. F. Young, A. Z. Csank, C. A. Froyd and D. McCarroll. 2010. Temporal stability in bristlecone pine tree-ring stable oxygen isotope chronologies over the last two centuries. *The Holocene* 20: 3-6.

BC Ministry of Environment. 1978. *The Soil Landscapes of British Columbia*, ed. K. W. G. Valentine, P. N. Sprout, T. E. Baker, and L. M. Lawkulich, 191 pp. British Columbia: Resource Analysis Branch.

BC Ministry of Environment. 2013. *British Columbia Groundwater Observation Network*. http://www.env.gov.bc.ca/wsd/data_searches/obswell/map/obsWells.html (Accessed August 2013).

Berkelhammer, M. B. and L. D. Stott. 2008. Recent and dramatic changes in Pacific storm trajectories recorded in $\delta^{18}O$ from Bristlecone Pine tree ring cellulose. *Geochemistry, Geophysics, Geosystems* 9:Q04008.

Brienen, R. J. W., G. Helle, T. L. Pons, J. Guyot, and M. Gloor. 2012. Oxygen isotopes in tree rings are a good proxy for Amazon precipitation and El Niño Southern Oscillation variability. *Proceedings of the National Academy of Sciences of the United States of America 109(42):*16957-16962.

Briffa, K. R., T. M. Melvin, T. J. Osborn, R. M. Hantemirov, A. V. Kirdyanov, V. S. Mazepa, S. G. Shiyatov, and J. Esper. 2013. Reassessing the evidence for tree-growth and inferred temperature change during the Common Era in Yamalia, northwest Siberia. *Quaternary Science Reviews* 72:83-107.

Brooks, J. R., H. R. Barnard, R. Coulombe, and J. J. McDonnell. 2010. Ecohydrologic separation of water between trees and streams in a Mediterranean climate. *Nature Geoscience* 3:100-104.

Brox, D., P. Procter, J. Pringle, B. Garrod, T. Morrison, and A. Saltis. 2004. The Seymour Capilano Twin Tunnels Project, Vancouver, BC. *2004 Tunnelling Association of Canada Proceedings.*

Bylhouwer, B., D. Ianson, and K. Kohfeld. 2013. Changes in the onset and intensity of wind-driven upwelling and downwelling along the North American Pacific Coast. *Journal of Geophysical Research – Oceans* 118:1–16*.*

Carton, J. A. 1984. Coastal circulation caused by an isolated storm. *Journal of Physical Oceanography* 14:114-124.

Clapp, R. B. and G. M. Hornberger. 1978. Empirical equations for some soil hydraulic properties. *Water Resources Research* 14(4): 601-604.

Crow, P. 2005. The influence of soils and species on tree root depth. *Forestry Commission* FCIN078.

Dansgaard, W. 1964. Isotopes in precipitation. *Tellus* 16:4.

Dawson, T. E. 1998. Fog in the California redwood forest: Ecosystem input and use by plants. *Oecologia* 117:476-485.

Dettinger, M. 2008. Pineapple Express Record 1948-2007. Unpublished Data.

Dettinger, M. 2004. *Fifty-two years of "Pineapple-Express" storms across the west coast of North America.* California: United States Geological Survey, Scripps Institutions of Oceanography for the California Energy Commission, PIER Energy-Related Environmental Research, CEC-500-2005-004.

Dettinger, M. D., D. R. Cayan, H. Diaz and I. Stewart. 2001. Decadal variations and trends in snowmelt and streamflow timing: Global and North American patterns in the 20th century. *Highest II Workshop*, Davos, Switzerland.

Di Lorenzo, E. 2013. NPGO index monthly averages from Jan-1950 to Jul-2013. http://www.o3d.org/npgo/npgo.php (Accessed July 2013).

Di Lorenzo, E., N. Schneider, K. M. Cobb, K. Chhak, P. J. S. Franks, A. Miller, J. C. McWillians, S. J. Bograd, H. Arango, E. Curchister. T. M. Powell, and P. Rivere. 2008. North Pacific Gyre Oscillation links ocean climate and ecosystem change. *Geophysical Research Letters* 35:L08607.

Dingman, S. L. 2002. Physical Hydrology. 2nd Edition. New Jersey: Prentice Hall. 464 pp.

Environment Canada. 2013. *Weather Office*. http://climate.weather.gc.ca/ (Accessed March 2013).

Gat, J. 1996. Oxygen and hydrogen isotopes in the hydrologic cycle. *Annual Review Earth Planetary Sciences* 24: 225–62.

Haught, D. R. W. 2010. *Runoff generation mechanisms in a steep first-order British Columbian watershed*. British Columbia: Simon Fraser University Master's thesis.

International Atomic Energy Association/ World Meteorological Organization. 2013. Global Network of Isotopes in Precipitation Database. http://www.iaea.org/water (Accessed August 2013).

Jansen, K., J. Sohrt, U. Kohnle, I. Ensminger and A. Gessler. 2013. Tree ring isotopic composition, radial increment and height growth reveal provenance-specific reactions of Douglas-fir towards environmental parameters. *Tree Ring Structure and Function* 27(1):37-52.

Johnstone, J. A., J. S. Roden, and T. E. Dawson. 2013. Oxygen and carbon stable isotopes in coast redwood tree-rings respond to spring and summer climate signals. *American Geophysical Union* doi: 10.1002/jgrg.20111.

Joint Institute for the Study of the Atmosphere and Ocean. 2012. *PDO Index*. http://jisao.washington.edu/pdo/PDO.latest (Accessed February, 2012).

Jouzel, J., F. Vimeaux, N. Caillon, G. Delaygue, G. Hoffman, V. Masson-Delmotte and F. Parrenin. Magnitude of isotope/temperature scaling for the interpretation of central Antarctic ice cores. *Journal of Geophysical Research* 18(D12):4361.

Lee, J. E. and I. Fung. 2008. "Amount effect" of water isotopes and quantitative analysis of post-condensation processes. *Hydrological Processes* 22:1-8.

Lepofsky, D., E. K. Heyerdahl, K. Lertzman, D. Schaepe, and B. Mierendorf. 2003. Historical meadow dynamics in southwest British Columbia: A multidisciplinary analysis. *Conservation Ecology* 7(3):5.

Lepofsky, D., K. Lertzman, D. Hallett and R.Matthews. 2005. Climate change and culture change on the southern coast of British Columbia 2400-1200 B. P.: A hypothesis. *American Antiquity* 70(2):267-293.

Li, J., S. Xie, E. R. Cook, G. Huang, R. D'Arrigo, D. Lui, J. Ma and X. Zheng. 2011. Interdecadal modulation of El Niño amplitude during the past millennium. *Nature Climate Change* doi: 10.1038/nclimate1086.

Loader, N. J., I. Robertson, A. C. Barker, V. R. Switsur, and J. S. Waterhouse. 1997. An improved technique for the batch processing of small wholewood samples to α-cellulose. *Chemical Geology* 36:313-317.

Madden, R. A., and P. R. Julian. 1994. Observations of the 40–50-day tropical oscillation: A review. *Monthly Weather Review* 122: 814–837.

Maechler, M. 2013. Package 'cluster'. http://cran.r-project.org/web/packages/cluster/cluster.pdf (Accessed April 2013).

Maloney, E. D. and J. T. Kiehl. 2002. MJO-related SST variations over the tropical eastern Pacific during Northern Hemisphere summer. *Journal of Climate* 15: 675-689.

Mantua, N. J., S. R. Hare, Y. Zhang, J. M. Wallace, and R. C. Francis. 1997. A Pacific interdecadal climate oscillation with impacts on salmon production. *Bulletin of the American Meteorological Society* 78: 1069-1079.

Martinez, L. 1996. Useful tree species for tree-ring dating. University of Arizona Laboratory of Tree-Ring Research. http://www.ltrr.arizona.edu/lorim/good.html (Accessed March 2011).

Mathis, J. T., R. S. Pickart, R. H. Byrne, C. L. McNeil, G. W. K. Moore, L. W. Juranek, X. Lui, J. Ma, R. A. Easley, M. M. Elliot, J. N. Cross, S. C. Reisdorph, F. Bahr, J. Morison, T. Lichendorf, and R. A. Feely. 2012. Storm-induced upwelling of high pCO_2 waters onto the continental shelf of the western Arctic Ocean and implications for carbonate mineral saturation states. *Geophysical Research Letters* 39:L07606-6.

McCarroll, D. and N. J. Loader. 2004. Stable isotopes in tree rings. *Quaernary Science Review* 23:771-801.

Mecke, M. and H. Ilvesniemi. 1999. The near-saturated hydraulic conductivity and water retention in coarse podzol profiles. *Scandinavian Journal of Forest Research* 14:391-401.

Meidinger, D. and J. Pojar. 1991*. Ecosystems of British Columbia. British Columbia*. BC Ministry of Forests. http://www.for.gov.bc.ca/hfd/pubs/Docs/Srs/SRseries.htm (Accessed August 2013).

Miller, D. L., C. I. Mora, H. D. Grissino-Mayer, C. J. Mocks, M. E. Uhle and Z. Sharp. 2006. Tree-ring isotope records of tropical cyclone activity, *Proceedings of the National Academy of Science USA* 103(39): 14294-14297.

Mitchell, T. 2004. Arctic oscillation time series, 1899- June 2002. http://jisao.washington.edu/data/aots/ (Accessed July 2013).

Mo, R. 2011. Pineapple Express. In *Meteorology today: An introduction to weather, climate and the environment*, ed. C. D. Ahrens, P. L. Jackson, and C. E. O. Jackson, 375 pp. Connecticut: Cengage Learning.

National Ocean and Atmospheric Administration (NOAA). 2003. *Monitoring Weather & Climate.* http://www.cpc.ncep.noaa.gov/products/precip/CWlink/daily_mjo_index/pentad.html (Accessed February, 2012).

NOAA, 2012. Pacific/ North American (PNA). http://www.cpc.ncep.noaa.gov/data/teledoc/pna.shtml (Accessed July 2013).

NOAA. 2013. Monthly teleconnection index: Pacific/ North American (PNA) pattern. ftp://ftp.cpc.ncep.noaa.gov/wd52dg/data/indices/pna_index.tim (Accessed July 2013).

Oosterbaan, R. J. and H. J. Nijland. 1994. Chapter 12: Determining the saturated soil hydraulic conductivity. In *Drainage Principles and Applications*, ed. H. P. Ritzema. The Netherlands: Institute for Land Reclamation and Improvement (ILRI) 16(2).

Pai, D. S., J. Bhate, O. P. Sreejith, and H. R. Hatwar. 2011. Impact of MJO on the intraseasonal variation of summer monsoon rainfall over India. *Climate Dynamics* 36:41-55.

Peterman, R. M. and B. Dorner. 2012. A widespread decrease in productivity of sockeye salmon populations in western North America. *Canadian Journal of Fisheries and Aquatic Sciences* 69:1255-1260.

Pojar, J., K. Klinka, and D.A. Demarchi. 1991. Chapter 6: Coastal Western Hemlock Zone, in *Ecosystems of British Columbia*. BC Ministry of Forests. http://www.for.gov.bc.ca/hfd/pubs/docs/Srs/Srs06/chap6.pdf (Accessed August 2013).

Porter, T. J., M. F. J. Pisaric, S. V. Kokelj, and T. W. D. Edwards. 2009. Climate signals in δ13C and δ18O of tree-rings from white spruce in the Mackenzie Delta region, northern Canada. *Arctic, Antarctic, and Alpine Research* 41: 497-505.

Roden, J. S., J. A. Johnstone, and T. E. Dawson. 2009. Intra-annual variation in the stable oxygen and carbon isotope ratios of cellulose in tree rings of coast redwood (Sequoia sempervirens). *The Holocene* 19(2): 189-197.

Sano, M., R. Ramesh, M. S. Sheshshayee, and R. Sukumar. 2012. Increasing aridity over the past 223 years in the Nepal Himalaya inferred froma tree ring $\delta^{18}O$ chronology. *The Holocene* 22(7): 809-817.

Saurer, M., P. Cherubini, and R. Siegwolf. 2012. Oxygen isotopes in tree rings of *Abies alba*: The climatic significance of interdecadal variations. *Climate and Dynamics* 105(D10):12461-12460.

Shu, Y., X. Feng, C. Gazis, D. Anderson, A. M. Faiia, K. Tang, and G. Ettl. 2005. Relative humidity record in tree rings: A study along a precipitation gradient in the Olympic Mountains, Washington, USA. *Geochimica et Cosmochimica Acta* 69:791-799.

Singer, M. B., J. C. Stella, S. Dufour, H. Piegay, R. J. S. Wilson, and L. Johnstone. 2013. Contrasting water-uptake and growth responses to drought in co-occuring riparian tree species. *Ecohydrology* 6(3): 402-412.

Sternberg, L. S. L. 2009. Oxygen stable isotope ratios of tree-ring cellulose: The next phase of understanding. *New Phytologist* 181: 553-562.

Thompson, D. W. J. no date. Indices of annular modes (ie., the AO and AAO). http://www.atmos.colostate.edu/ao/Data/ao_index.html (Accessed July 2013).

Trenberth, K. E. 1997. The definition of El Niño. *Bulletin of the American Meteorological Society* 78: 2771-2777.

University Corporation for Atmospheric Research. 2012. *TNI (Trans-Niño Index) and N3.4 (Niño 3.4 Index).* http://www.cgd.ucar.edu/cas/catalog/climind/TNI_N34/index.html#Sec5 (Accessed February, 2012).

Wang, T., A. Hamann, D. Spittlehouse, and S. N. Aitkens. 2006. Development of scale-free climate data for western Canada for use in resource management. *International Journal of Climatology* 26(3): 383-397.

Yamaguchi, D. K. 1991. A simple method for cross-dating increment cores from living trees. *Canadian Journal of Forestry Research* 21:414-416.

Zhang, Y., J. M. Wallace, D. S. Battisti. 1997. ENSO-like interdecadal variability: 1900-93. *Journal of Climate* 10: 1004-1020.

3.7. Appendix. Tree ring α-cellulose $\delta^{18}O$ values for annual, earlywood and latewood samples from a Douglas-fir (DF3a) in the Capilano River Regional Park in North Vancouver, British Columbia.

Measured values are underlined, and calculated values are in regular front.

Year	Annual[1]	Earlywood	Latewood
1960	22.6	22.9	22.3
1961	20.2	19.3	21.1
1962	19.2	18.3	20.3
1963	19.9	21.9	18.7
1964	18.9	24.6	16.8
1965	22.2	18.7	25.6
1966	22.7	21.3	23.5
1967	23.5	22.4	24.8
1968	25.8	22.2	28.0
1969	23.9	19.1	27.4
1970	22.8	21.7	24.3
1971	23.4	23.1	23.9
1972	24.9	23.9	26.2
1973	25.5	25.1	26.2
1974	24.6	23.7	25.3
1975	25.1	24.5	25.4
1976	22.1	23.2	21.8
1977	23.5	24.2	23.4
1978	22.4	24.0	21.5
1979	23.8	23.3	24.7
1980	23.9	22.5	24.8
1981	21.5	23.6	21.0
1982	24.2	23.2	24.7
1983	22.8		
1984	22.9	21.4	25.2
1985	24.8	24.6	25.1

Year	Annual[1]	Earlywood	Latewood
1986	25.3	24.6	26.3
1987	26.3	26.0	26.6
1988	24.4	22.8	26.0
1989	23.7	23.2	24.0
1990	24.3	23.7	24.9
1991	24.9	23.5	25.5
1992	24.0		
1993	23.3	21.8	25.6
1994	26.2	25.6	26.8
1995	26.0	26.3	25.6

[1] Annual $\delta^{18}O$ measurements are from tree core DF3b.

Chapter 4.

General Conclusion

Making decisions in an uncertain climate requires a comprehensive understanding of past conditions, which inspired my research to investigate the use of historical and proxy data as a tool for climate change adaptation and mitigation. In Chapter 2, I identified that PE storms have significantly higher upper quartile precipitation and stream discharge means than non-PE storms, as well as significantly enriched $\delta^{18}O$ signatures. The annual frequency of PE storms is 0-7 storm days/year (average of 1.5 days). However, they can contribute up to 17% of the annual precipitation and 37% of the annual streamflow over a given year. Of all the climate oscillations considered, PE frequency is negatively correlated to the Madden Julian Oscillation. The annual PE storm maxima are significantly correlated with both PE frequency and annual average temperature, with warmer years producing a greater number of PE storms of higher intensity. The arrival of concurrent PE storm systems over a short period of time creates antecedent saturated soil conditions that can trigger precipitation-induced natural hazards, such as flooding and debris flows, and thus significantly increase the potential risks to the public. The characteristic enriched oxygen isotope signature of PE storms allows us to quantitatively define individual storm systems based on their moisture source. Therefore, oxygen isotopes in precipitation have the potential to be used as a climate research tool to identify storm types, track storm characteristics and gather statistics on the frequency, magnitude and variability of PE storms.

In Chapter 3, I developed a tree ring oxygen isotope record for Vancouver, 1960-1995. The record can be divided into two different phases. First, prior to 1970, the stable isotope record is highly variable. Second, post-1970, when the stable isotope record is more enriched and consistent from year-to-year. The timing of the shift corresponds to temperatures increases that were recorded at a meteorological station in nearby

Washington State. Isotopic variability was not correlated with source water (PE) variables, and the influence of individual climate oscillations was difficult to isolate because of the multiple timescales over which climate oscillations operate. The earlywood $\delta^{18}O$ values, which are the most likely to pick up precipitation associated with winter months, are correlated with the Arctic Oscillation while the latewood $\delta^{18}O$ values are correlated with lower latitude oscillations like the Madden Julian Oscillation and the North Pacific Gyre Oscillation. The oxygen isotope record for Vancouver is significantly correlated to tree ring isotopes in the Northwest Territories, and both records have an inverse relationship with records from California. My results are consistent with other studies that suggest the presence of a boundary between northern and southern oceanographic conditions off the coast of British Columbia, such as Peterman and Doern (2012) and Lepofsky et al. (2005). The boundary has been known to shift over time, and is related to changes in oscillatory climate behaviour and Pacific salmon productivity.

The success of this study has raised many important research questions that could be addressed by subsequent research. I recommend the establishment of a bulk monthly or storm-by-storm basis isotopic sampling program which could provide valuable information about temperature, storm trajectory, moisture source, and other types of key storm characteristics. My results suggest that the isotopic signature of a storm can get lost to run-off or be dampened by isotopic mixing in the soil, so it is imperative to capture the precipitation as it falls. Another interesting avenue to explore would be identifying the isotopic composition of fog in the Capilano watershed, and calculating the relative contributions of fog and precipitation to the total annual tree ring $\delta^{18}O$ composition.

I would also recommend the development of a pooled oxygen isotope record for Vancouver, BC that extends back in time far beyond 1960. A pooled record will be a better representation of average stand conditions and would help to resolve whether the two phases (prior and post 1970) in my tree ring $\delta^{18}O$ record from the Capilano Watershed actually represent a change in climate that is shared across the region. As well, increasing the record length will make it more comparable with the California record, Northwest Territories record, and low-frequency oscillations such as the Pacific Decadal Oscillation.